CHALMERS

Optimisation of Composite Structures Using a Growth Algorithm

Master's Thesis in the Master's programme in Advanced Engineering Materials

MUHAMMAD ABDULLAH BEG

Department of Applied Mechanics
Division of Material and Computational Mechanics
CHALMERS UNIVERSITY OF TECHNOLOGY
Göteborg, Sweden 2011
Master's Thesis 2011:48

MASTER'S THESIS 2011:48

Optimisation of Composite Structures Using a Growth Algorithm

Master's Thesis in the Mater's programme in Advanced Engineering Materials

MUHAMMAD ABDULLAH BEG

Department of Applied Mechanics
Division of Material and Computational Mechanics
CHALMERS UNIVERSITY OF TECHNOLOGY
Göteborg, Sweden 2011

Optimisation of Composite Structures Using a Growth Algorithm
Master's Thesis in the Master's programme in Advanced Engineering Materials
MUHAMMAD ABDULLAH BEG

Master's Thesis 2011:48
ISSN 1652-8557
Department of Applied Mechanics
Division of Material and Computational Mechanics
Chalmers University of Technology
SE-412 96 Göteborg
Sweden
Telephone: + 46 (0)31-772 1000

Name of the printers / Department of Applied Mechanics
Göteborg, Sweden 2011

Optimisation of Composite Structures Using a Growth Algorithm
Master's Thesis in the Master's programme in Advanced Engineering Materials
MUHAMMAD ABDULLAH BEG
Department of Applied Mechanics
Division of Material and Computational Mechanics Chalmers University of Technology

ABSTRACT

This thesis work deals with the development of an algorithm that works together with the finite element method to optimize the fibre orientation and ply thickness of a composite material. The algorithm is developed for symmetric lay-up of orthogonal plies so that the coupling matrix is zero, i.e., there is no extension-twisting or bending-shearing coupling. The results in the report are shown for composites made of orthogonally held graphite fibres and an epoxy matrix. Properties of the composite material are calculated using Rule of Mixture (ROM) and classical laminate theory. The thickness and fibre orientation inside each element are considered as independent variables. The fibres are aligned in the principal stress directions in every element. The maximum strain criterion is used to control the fibres amount, or in other words, increase in the element thickness. This algorithm is inspired from the natural bone growth in a living organism in which only the certain parts of the bone grow and densify that are under a high state of stress. The thesis work in carried out using the MATLAB based finite element tool "CALFEM" and the optimisation algorithm is also written in MATLAB. The algorithm is then tested against several load cases and the results are discussed.

Key words: Fibre orientation; Topology optimization; Finite Element Method; Symmetric lay-up; Classical Laminate Theory

Contents

1 INTRODUCTION 1

1.1 Literature Review 1

1.2 Micro and Macro mechanics of laminates 8

1.3 Failure criteria for composite materials 12

1.4 Finite element analysis of composite 12

2 METHOD 15

3 NUMERICAL EXPERIMENTS 21

3.1 Plate under uniaxial loading 21

3.2 Plate under point loading 25

3.3 Trapezoid under uniaxial loading 29

3.4 Plate under pure shear loading 33

3.5 Plate with hole under tension 37

3.6 Plate under multiple loads 41

4 ANALYSIS 45

5 DISCUSSION AND CONCLUSIONS 49

6 FUTURE WORK 51

REFERENCES 53

Preface

This thesis work is carried out Swerea SICOMP, Mölndal Sweden. I would like to thank my supervisor Maciej Wysocki for believing in me, guiding me at every step and providing me the resources required for the thesis work at Swerea SICOMP, Mölndal. Thanks to thank Alan André, Erik Marklund and Robin Olosson for helping me whenever I asked for. Special thanks to the people working in Swerea IVF and Swerea SICOMP to provide a friendly working environment.

Special thanks to the fellow thesis workers, Robert Ruppi, Muhammad Dilawar Hayat, Keyvan Amiri, Xu and Johan Wallin who made my stay at Swerea more enjoyable.

Last but not least thanks to Fredrik Larsson for being such a wonderful teacher in the FEM-application course which helped me a lot during my thesis work and otherwise as well for being my examiner and guiding me during my thesis work.

Göteborg June 2011

Muhammad Abdullah Beg

1 Introduction

Composite materials are replacing metallic counterparts in many structural applications. This is due to their low weight together with high strength and high stiffness. Their properties can be tailored for specific design requirements due to their anisotropic properties. This can be achieved by changing the stacking directions, changing stacking sequence and/or thickness of fibres at a particular position in a component. However due to increase number of design variables, the mechanical complexity of such material will also increase. The mechanical behaviour of such a material is more challenging to determine and model than that of conventional materials, i.e. failure mechanisms in composites such as fibre breaking, matrix cracks, fibre compressive failure and matrix crushing and different couplings of normal force, shear force and moments will change due to different stacking sequences.

Optimisation is one such problem in which the techniques used for isotropic materials may not be effective in the case of composite materials. For instance, gradient methods are suspected to fail in case of composite materials. The reason is that gradient methods consider the design variable as a continuous variable whereas the number of plies in a composite is a discrete variable. Moreover, for gradient methods, the initial guess should be good enough so that the method should converge to the global minimum which is difficult for composites. The reason for these problems in composite materials is the multiple ply directions. For complex load cases plies need to be rotated in every element. Plies in a certain direction minimize the objective function locally for an element but not globally. Unfortunately, increasing the number of design variables also increases the number of local minima and methods such gradient methods, Genetic algorithm and Simulated annealing may fail to provide optimal values.

1.1 Literature Review

Optimisation is a science to determine best possible solutions using set of mathematical equations that represent a physical system. There are numerous examples of intrinsic optimisation of physical systems in our daily life i.e. a droplet of water, under zero gravity, is a perfect sphere which has the smallest surface area for a given volume, arrangement of atoms in a unit cell to have minimum energy level, selection of material of an aircraft wing and scheduling of flights by an airline. An optimisation problem in engineering applications is generally a set of independent

variables defined in form of an equation or a set of equations called "objective function". In an optimisation problem the purpose is to maximise or minimize the value of objective function. There can be restriction on the objective functions which are known as constraints. Consequently, an optimisation problem is all about maximisation or minimisation of an objective function, which is an equation in terms of an independent variable, with certain constraints on the values of the independent variable [1, 2, 3, 4]. An optimisation problem with constraints can be represented mathematically as:

$$minimize\ f(x) \tag{1.1}$$
$$subject\ to\ c_i\ (x)\ = 0, i = 1, 2, 3 \ldots m$$
$$c_i(x)\ \geq\ 0\ for\ i = m + 1, m + 2, .. m',$$

where $f(x)$ is the objective function to be minimized and $c_i(x)$ is constraint function and together they form the problem function. The problems in which there are no constraints on objective function are called unconstraint problems [2, 3] and can be represented as:

$$minimize\ f(x) \tag{1.2}$$
$$x^U{}_i = -x^L{}_i = \infty,$$

where $x^U{}_i$and $x^L{}_i$ are upper and lower bounds on the design variable. Optimisation problems can also be characterized according to the structure of the problem. Convex optimisation problem is one in which both the objective function and the constraints form a convex set. An optimization problem can be a convex problem if minimization objective function,$f(x)$ as well the space, X, in which the independent variable, x, is defined are convex function and convex set respectively [4]. Mathematically:

$$\text{minimize f(x)} \tag{1.3}$$
$$\text{such that x} \in \text{X, X} \rightarrow \text{ R.}$$

For convex problems, if a minimum exists then it is a global minimum and for strictly convex problems if there exist a minimum then it is unique. Linear programming is one of the most important branches of convex programming which consists of various problems in which both the objective functions and the constraints are linear functions of independent variable. In these problems every constraint defines a line which divides feasible and infeasible regions. All the points inside the feasible region satisfy all the constraints of the problem [3]. These problems can be solved using using Simplex method. The method requires introduction of slack variables to convert the

problem into a standard form. This method searches for the minimum value of the objective function along the boundaries of the feasible region and terminate when a minimum value or an unbounded edge is reached [3]. Integer linear program is a variant of linear programming in which the design variable can only have integer or discrete values. Such problems that can take values of only 0 and 1 can be solved by implicit enumeration. Methods that can be used to solve mixed integer problems are Branch and Bound algorithms, Genetic algorithm, Gomory cut method and Simulated Annealing [3]. For constrained linear problems, it is necessary to satisfy Karush, Kuhn and Tucker (KKT) condition [3].

For nonlinear problem different types of methods are employed which can broadly categorized as (i). Direct search methods, (ii). Gradient methods and (iii). Second order methods. Direct search methods are methods that are use for problems which have discontinuous objective function, $f(x)$ and where it is assumed a continuous, gradient discontinuous, or a complex function of design variables. These heuristic search methods are based on geometric intuition which provides no performance guarantees other than comparison of results. Theoretically, direct search techniques are based on mathematical foundation and provide convergence under restricted conditions. S^2 or simplex search method is a heuristic search method. One of the techniques is to divide the search space into regular grids and different techniques are used to shrink the search area around the solution. The problem with this technique is the computational time. A modified version of this technique is to consider a base point in the search space and consider the performance criteria of points with respect to the base point. Another important heuristic direct search technique is Hooke-Jeeves pattern search method which searches for optimal design variable in fixed set of directions. In this method one variable is chosen at a time and the design space is search in the coordinate direction. It works fine for the objective functions with spherical symmetry but not for functions which are distorted or elongated- in that case it doesn't converge even after infinite number of shorter and shorter steps. Powell's conjugate direction method is one of the most successful direct search method which is based on the quadratic nature of the objective function. Since a quadratic function is the simplest type of nonlinear objective function and nonlinear functions can be approximated as quadratic functions using Taylor's expansion near the optimal design variable, Powell's method converges to optimality in finite number of searches. However like other direct search methods this method is also slower than

gradient based methods [2]. Some other direct search methods are Spendley, Hext and Himsworth's method, Nelder and Mead's, Davidon's cubic interpolation method and Fibonacci search. Details about these can be studies in [3, 5]. Setoodeh et al. [7] used a Quadratic programming technique to design variable stiffness laminates.

For first order gradient methods it is assumed that the first derivative of objective function $\nabla f(x)$ exists. The general form of gradient based iteration process is [6]:

$$f_1(x) = f(x^k) + \boldsymbol{\nabla} f(x^k)^T (x - x^k), \tag{1.4}$$

where $f_1(x)$ is the updated objective function, $f(x^k)$ is the previous value of the objective function $\boldsymbol{\nabla} f(x^k)$ is the gradient of objective function at x^k and $(x - x^k)$ is the search direction. Steepest descent method or Cauchy's method is a simple gradient method technique. The gradient $\boldsymbol{\nabla} f(x^k)$ represent the direction of the most locally increasing direction, while $-\boldsymbol{\nabla} f(x^k)$ represents the direction of the most locally decreasing direction. This is quite clear since [3]

$$\boldsymbol{\nabla} f(x^k)^T (x - x^k) \; = \; -\left|\left|\boldsymbol{\nabla} f(x_k)\right|\right|^2 < 0, \tag{1.5}$$

and the new point is given using,$x^{k+1} = \; x^k - \; \alpha(x - x^k)$, where α is the step size in the search direction chosen in such a way that x^{k+1} minimizes the function's value $f_1(x)$ in the direction of $-\boldsymbol{\nabla} f(x^k)$. Each search direction is orthogonal to the previous direction which gives a zigzag and thus slower convergence rate [3]. Another reason of slower convergence is that magnitude of gradient decreases with every iteration [2]. The method is good when the condition number of the Hessian matrix $\boldsymbol{\nabla}^2 f$ is closer to unity or in other words the contours of objective function are circular [2, 3]. Thus the steepest descent method fails for highly nonlinear problems. A example of this drawback is shown by Herrmann [8] performing a test on Rosenbrock Banana function. Further details about steepest descent method can be found in [2, 3].

Second order methods are used in order to get a better global direction than steepest descent method. These methods employ second order Taylor series to get a quadratic approximation of objective function. This approximation is used to determine a next iteration point x^{k+1} for which the gradient of approximation is zero. This type of iterative method is called Newton's method. The next point in the search direction is calculated as [2]

$$x^{k+1} = \; x^k - \; \boldsymbol{\nabla}^2 f(x^k)^{-1} \boldsymbol{\nabla} f(x^k). \tag{1.6}$$

Since a quadratic approximation is used, Newton's method converges faster than first order methods. However, the method may not converge to the global optimal unless the starting point is close to optimum. The reason are that for highly nonlinear problems even the quadratic approximation may be a poor approximation and if the Hessian at $x^k, \nabla^2 f(x^k)$ is singular or not positive definite than approximation function may not have a minimum, i.e. a saddle point or a flat function. One method to overcome this problem is modified Newton method is which a step size parameter α^k is introduce, as in Cauchy's method. The new iteration point is then given as

$$x^{k+1} = x^k - \alpha^k \nabla^2 f(x^k)^{-1} \nabla f(x^k) \tag{1.7}$$

Marquardt's method is another modification that could be applied when the Hessian matrix is singular. It incorporates Cauchy's method when the iteration point is far from optimum and then uses Newton's method near the optimum. The new search direction becomes

$$d^k = -(\nabla^2 f(x^k) + \lambda \boldsymbol{I})^{-1} \nabla f(x^k), \tag{1.8}$$

where λ is used to control both direction of search and $\boldsymbol{I}$ is identity matrix. The value of λ is chosen larger than the absolute minimum Eigen value of Hessian, $\nabla^2 f(x^k)$ [6]. Quasi-Newton methods like Davidon-Fletcher-Powell or DFP method and BFGS(Braydon, Fletcher, Goldfarb and Shanno) method approximate the curvature of nonlinear functions without actually calculating the Hessian and instead use the first order information of the objective function. A detailed study about second order gradient methods can be found in [1, 2, 3, 6]. Modified feasible direction is a modified steepest descent method which keeps track of gradient of objective functions, constraints and search directions in the previous iteration. Topal and Uzman [9,10] have used modified feasible direction method for optimising the laminated plates for buckling loads. Lindgaard and Lund [11] also used gradient based method to optimise composite structures against buckling loads.

Simulated annealing (SA) is a generalization of Monte Carlo simulation. It is a direct search method which is based on annealing of metals and glasses to relieve them from residual stresses. A general SA problem can be represented as

$$minimize\ f(\boldsymbol{x}) \tag{1.9}$$

$$subject\ to\ l_i \le x_i \le u_i, i = 1\ to\ n.$$

Annealing is process in which metal or glass parts are heated to a certain high temperature and then cooled in a controlled environment in order to allow the atoms

to rearrange themselves in a lower energy state and attain stable equilibrium. For a thermodynamics system, the probability of change in energy state for a given temperature, T is given by Boltzmann's probability distribution function

$$p(\Delta E) = e^{-\Delta E/kT}, \quad (1.10)$$

where ΔE is the activation energy, T is temperature and k is Boltzmann's constant. In an optimisation problem, an initial state of temperature, which is analogous to design variable is set a very high value and the Boltzmann's constant, k is set to a value, and may be chosen as 1. A vector of step sizes is chosen to find change in energy level, which is analogous to objective functions, along the coordinate directions. At each temperature the change is objective function is calculated along the coordinate directions. If the change shows a decrease in function value, it is accepted and the new design variable is calculated at that function value. If the function value is shows an increase in function value it is accepted if the probability of its occurrence is less than a certain desired value. This allows the optimisation problem not to get stuck to local minima. At the end of iteration the step size is updated. In order to apply this technique, one has to describe initial temperature, the state space, the acceptance probability function, energy/neighbour generator function, annealing schedule and number of iterations at each temperature. The difficulty is that there is no general way to find the best choices of factors and these choices are different of different problems. Akbulut and Somez have used an SA technique from minimum thickness of composite laminates [12]. A detailed discussion on Simulated Annealing (SA) is given [3].

Genetic algorithm (GA) is nature based optimisation technique. It is a computational technique that simulates the evolution process of genetic reproduction-the strategy is that the fittest shall survive. This technique can be used for discrete as well as continuous design variables. This technique can converge to a minimum even when the design domain is very large. The general form for an optimisation problem is given in the same way as for an SA optimisation problem. In a GA problem each variable x_i is encoded as a binary code of some specific number of bits, say m. The feasible interval of variable x_i is divided into $2m-1$ intervals. In the first step an initial population is created using attaching the binary values of each variable's bit value end to end with those of other variables. The bit size of each member of the population is then $m*n$, where m is the bit size of variable and n is the number of design variables.

The size of the population to be generated is a matter of experimentation. In the next step, each of the members is decoded and the objective function values for them are evaluated. The function values are referred to as fitness values in GA. Once the population's fitness values are determined, the next step is to make a pool of mating parents. The selection of the genes for reproduction is carried by replacing the weaker members, members with low fitness values, using stronger members. There are several ways in which this replacement can be done. One of the schemes could be a simulated roulette wheel which randomly replaces the weak members using stronger members. The selected parents are then crossover. One of crossover technique is to replace a variable at a certain position in a parent's genes with a corresponding variable in the other mating parent's genes to give birth to two offspring. Some researchers have used this technique with more than two parent genes as well. Once a suitable population of children members in produced, it is checked if the children are too identical to each other. If they are too identical, they will slow down or even stop the evolution. This is prevented by mutation. The purpose of mutation is to introduce diversity in the population. Every bit in a child is given a random value which determines whether or not the bit will be modified in the process. This type of mutation is called biological point mutation. Other mutation techniques are also available such as, floating point mutation, inversion, scramble and swap. After mutation the population is evaluated. Now, once again of each member of the population is evaluated on the basis of their fitness values. Like before the highest the fitness value, the fittest the member is for next generation. This step is referred to as Evaluation. If the number of populations to be generated is reached then process is stop, other using the new population as parent population the process is started over again. This process is continued until the preset number of populations to be generated is reached. However there are problems with GA as well. First of all, it has no theoretical background and at times the experimental results challenged the accuracy of this technique. Furthermore there is a divided opinion about the preference of crossover and mutation. Different parameters such as population size, crossover probability and mutation probability have effects on the final results. Composite structures are optimised using GA Herrmann, Naik et al., Legrand et al., Almeida and Awruch and Paluch el al. [8, 13, 14, 15, 16]. Details about GA can be studied from [17].

1.2 Micro and Macro mechanics of laminates

A laminate is made up of several lamina stacked in the thickness direction. Thus to understand the behaviour of a laminate one first needs to have knowledge about the micromechanics of a single lamina. The properties of lamina depend upon a variety of variables such as the volume fraction of fibre and matrix. These properties are affected by the voids present inside the composite material. e.g. lower shear stiffness and strength, compressive strength, transverse tensile strength, fatigue resistance and moisture resistance. There are four independent elastic constants for a unidirectional transversely isotropic ply:

- Longitudinal or axial Young's modulus, E_{11}
- Transverse Young's modulus, E_{22}
- In-plane shear modulus G_{12} and
- Major Poisson's ratio, ν_{12}.

There are different models to calculate these elastic constants. Rule of mixture is a good approximation for longitudinal direction, while the Reuss model (which assumes equal transverse stresses in fibre and matrix) is good to calculate transverse moduli. However, both of these models are not suitable for transverse or shear moduli as they underestimate the mechanical properties in transverse direction. Semi-Empirical model like Halphin-Tsai is widely used obtain in plane shear and transverse moduli. Details about different models can be studied in any book on composite mechanics, e.g. [18, 19, 20]. In the algorithm developed in this thesis strength of material approach or rule of mixture is used to calculate the elastic constants. Once the elastic constants are determined, compliance matrix for an orthotropic composite material in the local coordinate system (axial and transverse fibre directions) is given as:

$$[\boldsymbol{S}] = \begin{bmatrix} 1/E_1 & -\nu_{12}/E_2 & -\nu_{13}/E_3 & 0 & 0 & 0 \\ -\nu_{12}/E_1 & 1/E_2 & -\nu_{32}/E_3 & 0 & 0 & 0 \\ -\nu_{31}/E_1 & -\nu_{23}/E_2 & 1/E_3 & 0 & 0 & 0 \\ 0 & 0 & 0 & 1/G_{23} & 0 & 0 \\ 0 & 0 & 0 & 0 & 1/G_{13} & 0 \\ 0 & 0 & 0 & 0 & 0 & 1/G_{12} \end{bmatrix}, \quad (1.11)$$

where E_3, ν_{32}, ν_{13}, G_{23}, G_{13} are out of plane elastic constants. Assuming that the thickness of the composite material is small, plane stress approximation is used to calculate stresses and strains. This approximation simplifies the calculations by

ignoring the out-of-plane stress. In such a case the reduced compliance matrix is given as

$$[\boldsymbol{S}] = \begin{bmatrix} 1/E_1 & -\nu_{12}/E_2 & 0 \\ -\nu_{12}/E_1 & 1/E_2 & 0 \\ 0 & 0 & 1/G_{12} \end{bmatrix}. \tag{1.12}$$

Thus strain-stress relationship can be written in the form:

$$\begin{bmatrix} \epsilon_1 \\ \epsilon_2 \\ \gamma_{12} \end{bmatrix} = [\boldsymbol{S}] \begin{bmatrix} \sigma_1 \\ \sigma_2 \\ \tau_{12} \end{bmatrix}, \tag{1.13}$$

where σ_1, σ_2, τ_{12} and ϵ_1, ϵ_2, γ_{12} are stresses and strains in axial, transverse and shear directions respectively. Conversely,

$$\begin{bmatrix} \sigma_1 \\ \sigma_2 \\ \tau_{12} \end{bmatrix} = [\boldsymbol{Q}] \begin{bmatrix} \epsilon_1 \\ \epsilon_2 \\ \gamma_{12} \end{bmatrix}, \tag{1.14}$$

$$[\boldsymbol{Q}] = [\boldsymbol{S}]^{-1},$$

where $[\boldsymbol{Q}]$ is the stiffness matrix of the composite lamina. The stresses and strains can be transformed in global coordinates using transformation reduced stiffness,$[\overline{\boldsymbol{Q}}]$, and compliance matrices, $[\overline{\boldsymbol{S}}]$, respectively, such that

$$\begin{bmatrix} \sigma_x \\ \sigma_y \\ \tau_{xy} \end{bmatrix} = [\overline{\boldsymbol{Q}}] \begin{bmatrix} \epsilon_x \\ \epsilon_y \\ \gamma_{xy} \end{bmatrix} \tag{1.15}$$

$$[\overline{\boldsymbol{Q}}] = \begin{bmatrix} \bar{Q}_{11} & \bar{Q}_{12} & \bar{Q}_{13} \\ \bar{Q}_{12} & \bar{Q}_{22} & \bar{Q}_{23} \\ \bar{Q}_{13} & \bar{Q}_{23} & \bar{Q}_{33} \end{bmatrix} = [\boldsymbol{T}]^{-1}[\boldsymbol{Q}]$$

$$where\ [\boldsymbol{T}]^{-1} = \begin{bmatrix} c^2 & s^2 & -2sc \\ s^2 & c^2 & 2sc \\ sc & -sc & c^2 - s^2 \end{bmatrix}$$

$$and\ c = \cos\theta\ \ and\ s = sin\theta$$

Conversely,

$$\begin{bmatrix} \epsilon_x \\ \epsilon_y \\ \gamma_{xy} \end{bmatrix} = [\overline{\boldsymbol{S}}] \begin{bmatrix} \sigma_1 \\ \sigma_2 \\ \tau_{12} \end{bmatrix} \tag{1.16}$$

$$and\ [\overline{\boldsymbol{S}}] = [\overline{\boldsymbol{Q}}]^{-1},$$

where $[\boldsymbol{T}]$ is the transformation matrix and θ is the rotation angle of fibres with respect to the global coordinate system. The rotation of coordinate system from local to global is shown in *Figure 1.1*. Further details about stiffness and compliance matrices and there transformation can be found in [18, 19, 20].

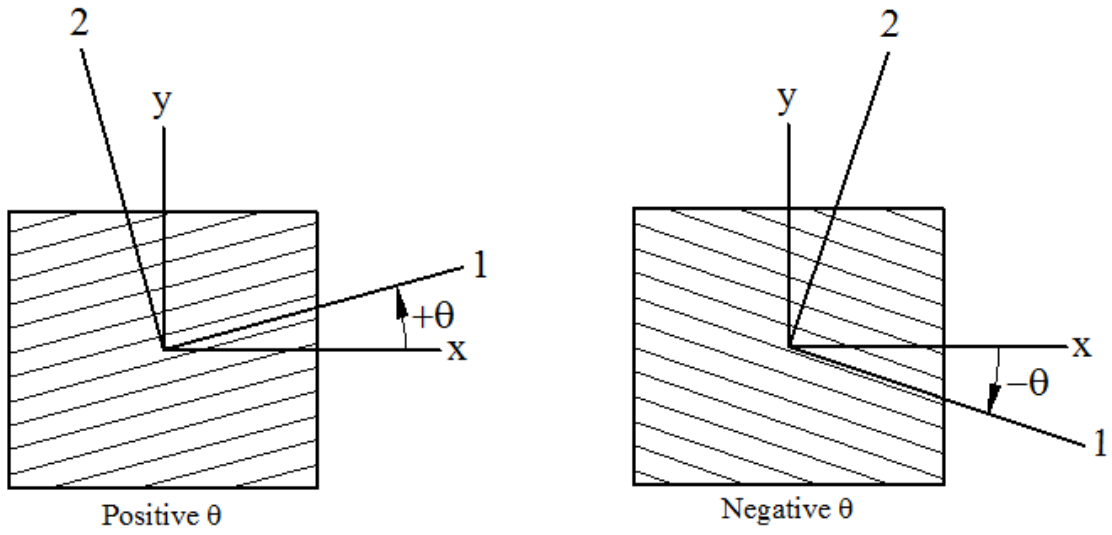

Figure 1.1 Rotation of coordinate system and sign convention for rotation angle

Since it is hard to find any use for a single ply composite the composites are usually multiply laminates. Thin composite laminates can be model using two dimensional theories. The simplest of these theories is Classical Laminate Theory (CLT), which is an extension of Kirchhoff plate theory and, ignores the out-of-plane stresses and strains. Thus it cannot be used for thick plates where out-of-plane strains are significant and at the edges of the thin plates. Consequently, this theory cannot take delamination into account. CLT is based on following assumptions

- Each ply is linearly elastic and orthotropic
- Laminates are perfectly bonded together
- Strain are small
- Through thickness strains are negligible
- Laminate thickness is constant and small as compared to in-plane dimensions of the plate

The response of composite material to in-plane forces and moments is determined by extensional stiffness matrix, [$\boldsymbol{A}$] coupling stiffness matrix, [**B**] and bending stiffness matrix, [**D**]. Extensional stiffness matrix, [$\boldsymbol{A}$] relates the in-plane forces, N_x, N_{xy} and N_{xy}, to the mid-plane strains, ${\varepsilon^0}_x$, ${\varepsilon^0}_y$ and ${\gamma^0}_{xy}$, and is calculated as

$$[\boldsymbol{A}] = \sum_{k=1}^{n} (\bar{\boldsymbol{Q}}_{ij})_k (z_k - z_{k-1}). \tag{1.17}$$

Bending stiffness matrix, [**D**] relates the in-plane moments, M_x, M_y and M_{xy}, to curvatures, $\varkappa_x$, $\varkappa_y$ and $\varkappa_{xy}$. It is calculated as

$$[\boldsymbol{D}] = \frac{1}{2}\sum_{k=1}^{n}(\bar{\boldsymbol{Q}}_{ij})_k({z_k}^2 - {z_{k-1}}^2). \quad (1.18)$$

Coupling matrix, [**B**] relates in-plane forces, N_x, N_{xy} and N_{xy}, to the curvatures $\varkappa_x$, $\varkappa_y$ and $\varkappa_{xy}$ and moments, M_x, M_y M_{xy}, to mid-plane strains, ${\varepsilon^0}_x$, ${\varepsilon^0}_y$ and ${\gamma^0}_{xy}$, and is calculated as

$$[\boldsymbol{B}] = \frac{1}{3}\sum_{k=1}^{n}(\bar{\boldsymbol{Q}}_{ij})_k({z_k}^3 - {z_{k-1}}^3). \quad (1.19)$$

Here in the three above equations $\bar{\boldsymbol{Q}}_{ij}$ is the stiffness matrix of k^{th} lamina, z_k and z_{k-1} are the distances of upper and lower surface of the lamina from the mid-plane or reference plane and n is the number of lamina in the plate. The notation is illustrated in *Figure 1.2*. The above three equations can be written together in matrix form as

$$\begin{bmatrix}\boldsymbol{N}\\ \boldsymbol{M}\end{bmatrix} = \begin{bmatrix}\boldsymbol{A} & \boldsymbol{B}\\ \boldsymbol{B} & \boldsymbol{D}\end{bmatrix}\begin{bmatrix}\boldsymbol{\varepsilon}^0\\ \boldsymbol{K}\end{bmatrix} \quad (1.20)$$

$$where\ \boldsymbol{N} = \begin{bmatrix}N_x\\ N_y\\ N_{xy}\end{bmatrix}, \boldsymbol{M} = \begin{bmatrix}M_x\\ M_y\\ M_{xy}\end{bmatrix}, \boldsymbol{\epsilon}^0 = \begin{bmatrix}{\varepsilon^0}_x\\ {\varepsilon^0}_y\\ {\gamma^0}_{xy}\end{bmatrix}, \boldsymbol{K} = \begin{bmatrix}\varkappa_x\\ \varkappa_y\\ \varkappa_{xy}\end{bmatrix}.$$

In case of symmetrical laminate there is no coupling effect so that the coupling matrix becomes zero, $[\boldsymbol{B}] = \boldsymbol{0}$. Consequently the in-plane moments will not produce any strain in the *mid- plane* and the in-plane stresses will not wrap or twist the *mid- plane*.

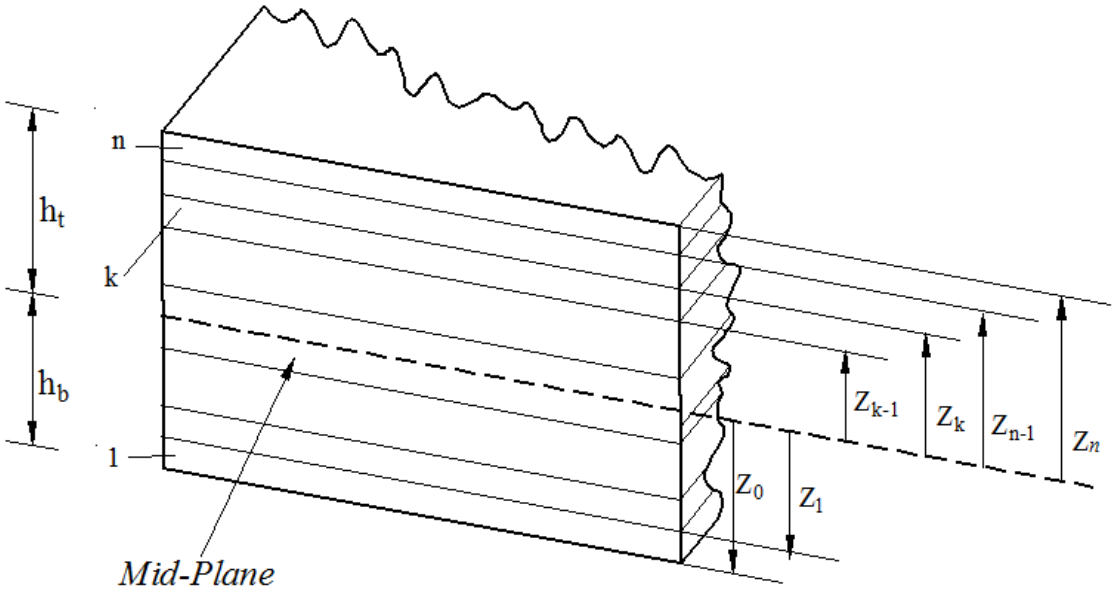

Figure 1.2 Laminate code used for a symmetric lay-up

In the algorithm developed in this thesis work a symmetrical laminates is considered. The affect of different lay-up strategies on [$\boldsymbol{A}$], [$\boldsymbol{B}$] and [$\boldsymbol{D}$] are discussed in detail in [18,19].

1.3 Failure criteria for composite materials

Composite materials can fail under different failure modes, i.e. fibre buckling, fibre breakage, matrix cracking, delamination or a combination of these failure modes. Several theories have been proposed in order to predict failure and its mode in composite materials but, so far, they are complicated and none of them is of practical interest. Instead, strength failure theories are used. These are simple and easy-to-implement theories. These theories include Qaudratic failure criterions like Tsai-Wu and Tsai-Hill failure criteria, maximum stress criterion and maximum strain criterion. These criteria have following limitations:

- These theories only predict the first ply failure. It is not necessary that the material will fail since other plies may redistribute the load. As the load will increase the rest of the plies will failure until the load is high enough to cause rapid failure.
- Mode of failure is not predicted
- Each criteria is applicable under certain limitations
- Some of the data required for these criteria are difficult to measure
- The criteria are applicable away from discontinuities e.g. holes, delamination, notches and edges.
- Maximum stress and maximum strain failure criteria for composites is not equivalent to those for isotropic materials. The reason is that stress and strain components along the orthotropic direction at a point in a composite material are compared with the allowable stresses and strains respectively and they are not necessarily maximum stresses and strains at that point.
- Maximum stress criterion is not equivalent to maximum strain criterion for composites.

Detailed discussion and mathematical representations about different failure criteria are given in [18, 19]. Due to ease of application and its validity for orthotropic materials under plane-stress conditions, maximum strain failure criterion is used in the algorithm developed in this thesis.

1.4 Finite element analysis of composite

Finite element method is a numerical technique to solve differential equations using certain approximation. The differential equation or equations represent a certain finite domain of a physical system. In a mechanical system finite element methods are used

to calculate stresses and strains in the system. The process consist of dividing the whole structure into small domains, called elements, is called meshing. Stiffness matrix [k] for each element is calculated and a global stiffness matrix [K] is constructed using all the element stiffness matrices. The boundary conditions, loads f and constraints, applied to the structure are transferred to the nodes. The displacements a at nodes are calculated using the following equation:

$$[K]a = f. \tag{1.21}$$

The displacements are used to find displacements inside an element using approximation functions [N], also called shape functions, by the following relationship:

$$u = [N]\delta, \tag{1.22}$$

where δ is the nodal displacement vector of the element. The nodal displacements can also be used to calculate element strain as

$$\epsilon = \tilde{\nabla}u = [B]\delta, \tag{1.23}$$

where B is the strain-displacement matrix and is the first derivative of element shape function with respect to the displacement variables.

$$[B] = \tilde{\nabla}N. \tag{1.24}$$

Element strains are then used to calculate stresses inside an element using Hooke's law

$$\sigma = E\epsilon, \tag{1.25}$$

where E is the stiffness matrix of the material.

Depending on the problem, the structure is divided in 1-D spring elements or beam elements, 2-D plate or 3-D brick elements. Sometimes, in order to simplify 3-D problem is solved as a 2-D problem using assumptions of plane stress or plane strain. Details about finite element methods can be studied in [22].

For thin composite materials under plane stress conditions it is typical to use 2-D four node quadrilateral element. However these elements cannot determine out-of-plane stresses and strains and thus can't be used to model the stress-strain state near and on free edges. Consequently, these elements can only be used in the regions where Classical Laminate Theory is valid. These elements are susceptible to shear locking which makes them excessively stiff and affects the accuracy of the results for plates with higher span-to-thickness ratio [23]. One of the techniques to over this problem is reduced integration which can result in another problem, hour glassing

modes. Hour glassing can be reduced using finer mesh or higher order elements [23, 24]. Details about different types of elements used in composite materials can be found in [24].

2 Method

In this thesis we develop an growth algorithm, which takes the idea from the growth of natural tissues such as bones and trees in which a bone is strengthened in the loading direction according to its loading conditions. In this study, a finite element code is coupled with this algorithm and provides information about the stress-strain state at element level. The growth algorithm adds ply material in each element in principal stress directions in discrete steps. To stop the optimisation loop maximum strain failure criteria is used as a design constraint. The amount of fibre in each direction is proportional to the stress state inside an element as well as related to the overall stress state of the material. After each step, another finite element calculation step is performed to obtain updated stress-strain state in the material. If the maximum strain in the material is below the maximum allowable strain then the algorithm returns the thickness values in each element and stops; otherwise, the procedure continues until the failure criteria is fulfilled in all elements. This is a kind of modification of *Last Ply Failure method* in which ply thickness is increased until the last ply is safe from failure. In this algorithm composite material is assumed to be free of all defects and carbon fibres are assumed to be uniformly distributed in a ply. Finite element calculations are done using MATLAB based FE-tool called CALFEM that is developed at University of Lund. The optimisation algorithm is written in MATLAB, where some of the original CALFEM files are modified to handle the element thicknesses as a vector. The structure is meshed using 4-node quadrilateral elements with 2 degrees of freedom at each node and linear shape functions are used for finite element approximations. As a consequence of plate element, either out-of-plane stress or strains cannot be calculated. This is not a problem in this case since Classical Laminate Theory (CLT) is employed here which ignores both out-of-plane stresses and strains. As a result this algorithm is valid for region away from the free boundaries. The opinion about region of validity of a 2-D analysis of a composite is divided. According to theoretical results of Pipes and Pigano that were later confirmed experimentally by Pipes and Daniels that for a symmetric angle-ply laminate the inter-laminar stresses are valid in a region of width equal to the laminate thickness from the free edges [24]. However the opinion is divided from 1 to 5 times the laminate thickness from the free edge depending upon the loading conditions and lay-up.

Firstly the structure to be optimised is modelled and the number of elements required along the two opposite sides is also defined here. This data is transferred to CALFEM meshing tool meshes the structure and divides the design domain into desired number of elements. It also provides the data regarding element degree of freedom, in-plane coordinates of the nodes in global coordinate system and degrees of freedom along the boundary of the design domain. Due to limitations on the CALFEM meshing tool only 4 sided polygons can be modelled and they need to be merged together to form other shapes. The coordinates of the elements are used to define the area of each element. Material properties for matrix defined in global coordinates which are isotropic macroscopically and are not affected by changing the coordinate system. However, since fibre composites are anisotropic in nature their properties will change with direction and are defined in local coordinates. The values of properties used for the analysis are given in the *Table 2.1*.

Table 2.1 Physical properties of Carbon fibre and epoxy

Mechanical properties of Carbon fibre	
Axial Modulus, E_{f1}	230 GPa
Transverse Modulus, E_{f2}	22 GPa
Major Poisson's ratio, υ_f	0.3
In-plane Shear Modulus, G_f	22 GPa
Axial tensile strength, σ_{1t}	2067 MPa
Axial compressive strength, σ_{1c}	1999 MPa

Mechanical properties of Epoxy Resin	
Axial Modulus, E_m	3.4 GPa
Poisson's ratio, υ_m	0.3
Shear Modulus, G_m	1.308GPa

A very small thickness is taken for the first isotropic FE analysis. The effect of thickness of the initial isotropic layer is explained later in the discussion. Next, the desired boundary conditions are applied on the nodes. A four node plane element is used for the analysis along with plane stress assumption. Due to these assumptions stresses normal to the plane are ignored which will have implications later when anisotropy is introduced. Using material properties of resin and plane stress assumption an isotropic material model is calculated for each element using the function "`plani4e_optimization`". This function is a slightly modified version of a CALFEM's function "`plani4e`". The element stiffness matrices are combined to form global stiffness matrix using the "`assem`" function. The FE system is now solved

using "`solveq`" to get nodal displacements and reactions at the boundaries. The nodal displacements are used to calculate element displacements using function "`extract`" which are used to calculate element stresses and strains using another function "`plani4s_optimization`". Integration rule 3 is used to find stresses and strains in each element. This is another function which is a modified version of CALFEM's function "`plani4s`". Element stresses are used to calculate principal stresses and their directions in each element which are simply the Eigen values and Eigen vectors of the element stress matrix. In a 2-dimensional analysis, two principal stresses are obtained which are orthogonal to each other.

Once the principal stresses and their directions are known, anisotropic ply thickness increment is added according to the stress state in every element. To increase the ply thickness a linear growth factor is employed. Since the plies are anisotropic in nature they can change the initial stress state in the structure. In order to avoid too much distortion of the stress-strain state, in the beginning a small amount of ply thickness is introduced along the principal directions. Both Principal stresses, depending upon their direction, are compared to the fibre strength in tension or compression. Then an anisotropic ply consisting of thickness equal to 1% of the thickness of isotropic layer times the ratio of principal stress to composite strength is added. Ply thickness increment can be mathematically represented as:

$$\Delta t_{1_n} = \eta * t_{n-1} * {}^{\sigma_1}/_{\sigma_a} \qquad (2.1)$$
$$\Delta t_{2_n} = \eta * t_{n-1} * {}^{\sigma_2}/_{\sigma_a},$$

where Δt_1 and Δt_2 are thickness increment in first principal direction, η is the percent growth factor used for ply thickness increment, n is the current time step, t_{n-1} is the total thickness in the previous time step, σ_1 and σ_2 are tensile or compressive stresses in first and second principal directions and σ_a allowable axial strength in tension or compression of the composite. Two growth factors, 1% and 100% are used for each case studied in this thesis and the results are compared. The contribution of orthogonal ply in one direction on ply increment in other direction is not considered as transverse strength of fibre, so ply's transverse strength, is very low as compared to axial strength. In the beginning, when anisotropic ply is introduced, t_{n-1} is equal to the thickness of isotropic layer. The material model for the anisotropic layers is determined using classical laminate theory. Since only in-plane deformations are

considered, only transformed reduced stiffness matrix $[\bar{Q}]$ is needed to be calculated. Rule of mixture is used to determine elastic moduli in different directions. Each ply is assumed to consist of 60% carbon fibre by volume and 40% epoxy by volume. This assumption is made due to manufacturing constraints on very high fibre volume in a composite. Thus the overall percentage of the fibre in the anisotropic layer is 60%. This also means that plies are assumed to be added symmetrically about the mid-plane. The stiffness model for the anisotropic plies is calculated using the function "`constitutivemodel`". Once the material model for plies is obtained it is added with that of isotropic middle plane according to following linear relationship

$$\bar{\mathrm{Q}}_{\mathrm{n}} = \left(\frac{\Delta \mathrm{t}}{\mathrm{t}_{\mathrm{n}}}\right) * \bar{\mathrm{Q}} + \left(1 - \frac{\Delta \mathrm{t}}{\mathrm{t}_{\mathrm{n}}}\right) * \bar{\mathrm{Q}}_{\mathrm{n-1}} \qquad (2.2)$$

$$\text{and } \mathrm{t}_{\mathrm{n}} = \Delta \mathrm{t} + \mathrm{t}_{\mathrm{n-1}},$$

where $\bar{\mathrm{Q}}$ is the material model of the orthogonal anisotropic plies, $\bar{\mathrm{Q}}_{\mathrm{n-1}}$ is the stiffness model of element for previous time step which, e.g. is isotropic material model for the first step, $\bar{\mathrm{Q}}_{\mathrm{n}}$ is material stiffness of the whole element, Δt is the thickness of orthogonal anisotropic plies, t_{n-1} is thickness of element in the previous time step (which in first step is equal to the thickness of isotropic layer) and t_n is total thickness. The step is schematically represented for an arbitrary element in *Figure 2.1*.

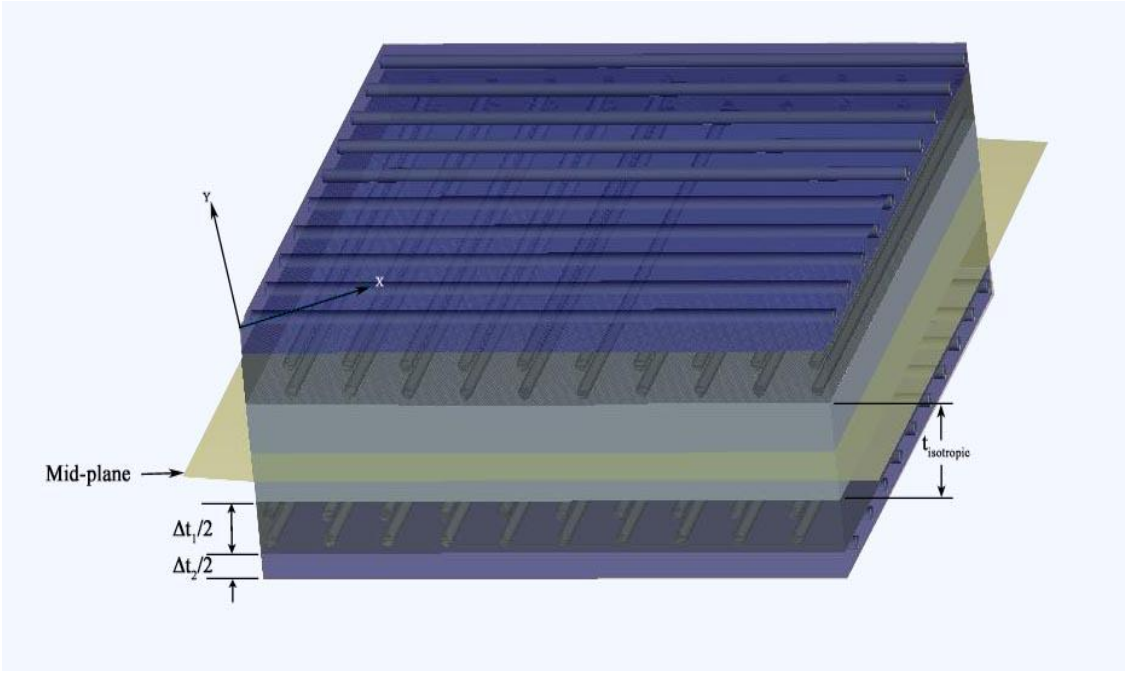

Figure 2.1 Introduction of anisotropic plies for an arbitrary element

Here $t_{isotropic}$ is thickness of the isotropic layer, $\Delta t_1/2$ and, $\Delta t_2/2$ are one half thicknesses of anisotropic plies in first and second principal directions respectively and *Mid-plane* is the plane of symmetry. Since the layup is symmetric the other halves of the ply thicknesses are above the mid-plane. The global coordinate system is represented using *X*-*Y*. Now this material model is used to calculate element stiffness matrix for elements using the function "`plani4e_optimization`". Element stiffness matrices are combined to form the global stiffness matrix using function "`assem`". The FE system is again solved using the boundary conditions similar to that of isotropic FE analysis. Nodal displacements and reactions at boundary nodes are obtained using "`solveq`" for the anisotropic analysis. It is observed that due to increased stiffness there is a decrease in nodal displacements. Once again, the nodal displacements are used to determine the element displacement using "`extract`". These displacements are then used to determine element stresses and strains in global coordinate system using function "`plani4s_optimization`". The stresses and strains in the local coordinate system which are eigen values of the stress and strain matrix respectively using function "`eigs`". These stresses and strains are the new principal stresses and strains of the structure. Maximum absolute value of the principal strain in the domain is compared to the maximum allowable strain. If the maximum strain for all elements is less than the maximum allowable strain then the process is stopped and the ply thickness in both principal directions and their orientations for all the elements are returned. If the failure criterion is not satisfied, current principal stresses are used to increase the ply thickness along the principal stress direction. The same procedure is employed to increase the ply thickness as before. The FE system is solved and principal stresses, their directions and principal strains are calculated. Maximum absolute strain of the system is compared to the maximum allowable strain. If the failure criterion is satisfied the code returns the values of ply thickness in each direction and their orientation otherwise the code continues to add material until the criterion is satisfied. The method used here for optimisation of ply thickness is exemplified using the flow diagram shown in *Figure 2.2*.

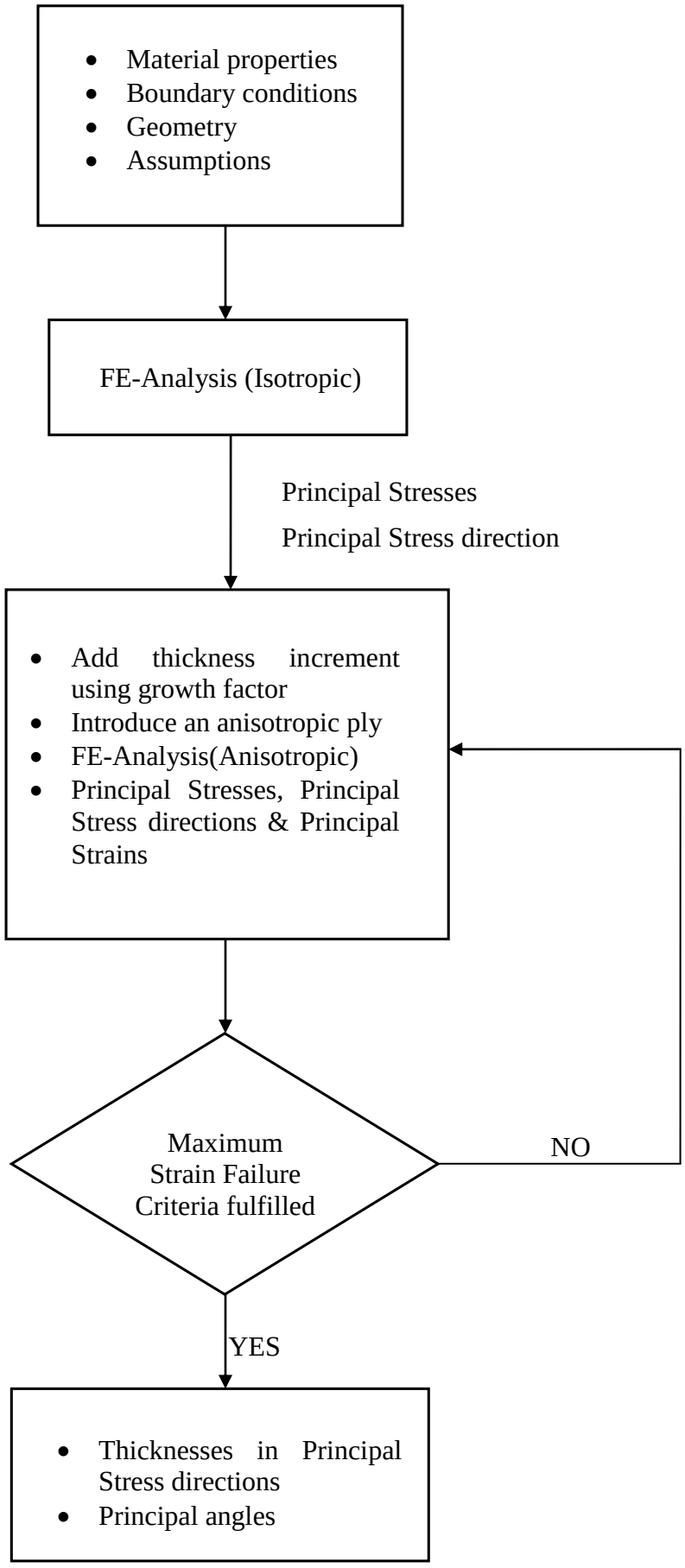

Figure 2.2 Flow chart of the optimisation process

3 Numerical Experiments

In this section a number of numerical experiments will be described. These consist of

- Square plate under uniaxial tension and compression
- Square plate under point loading
- Trapezoidal plate under uniaxial tension
- Square plate under pure shear load
- Plate with a hole in the middle under uniaxial tension
- Square plate under mixed loading

3.1 Plate under uniaxial loading

In this case a square 5x5cm plate under uniaxial tension and compression is considered to benchmark the algorithm. Due to symmetry conditions only a quarter of the plate is considered for analyses. A uniform force of 500kN is applied on the right side of the plate while the plate is constraint in x-direction on left side and in y-direction at the bottom as shown in *Figure 3.1*. Initial principal stress state for this loading condition for coarse mesh is also shown in *Figure 3.1*. *Table 3.1* shows the number of elements used for the analyses, applied load, the maximum and minimum thicknesses obtained from each analysis, total volume and computation time for uniaxial tension and uniaxial compression using a small growth factor (in first two analyses) and uniaxial tension with 100% growth factor(in last analysis) with 25 elements. The results for these analyses are shown in *Figure 3.2-Figure 3.4*. An element in *Figure 3.2* is marked '*a*' which shows rotation of principal stresses. The reason for this behaviour is discussed in Chapter 4, Analysis.

Table 3.1 Number of elements, applied load, maximum thickness, minimum thicknesses, total volume and computation time for each calculation for a square plate under uniaxial loading

Number of elements	Growth factor, η	Load	t_{max} [mm]	t_{min} [mm]	Volume [mm^3]	Computation time [seconds]
25	1%	500000N	15.94	15.94	9.98	119
25	1%	-500000N	16.00	16.00	10.01	103
25	100%	500000N	15.94	15.94	10.08	3

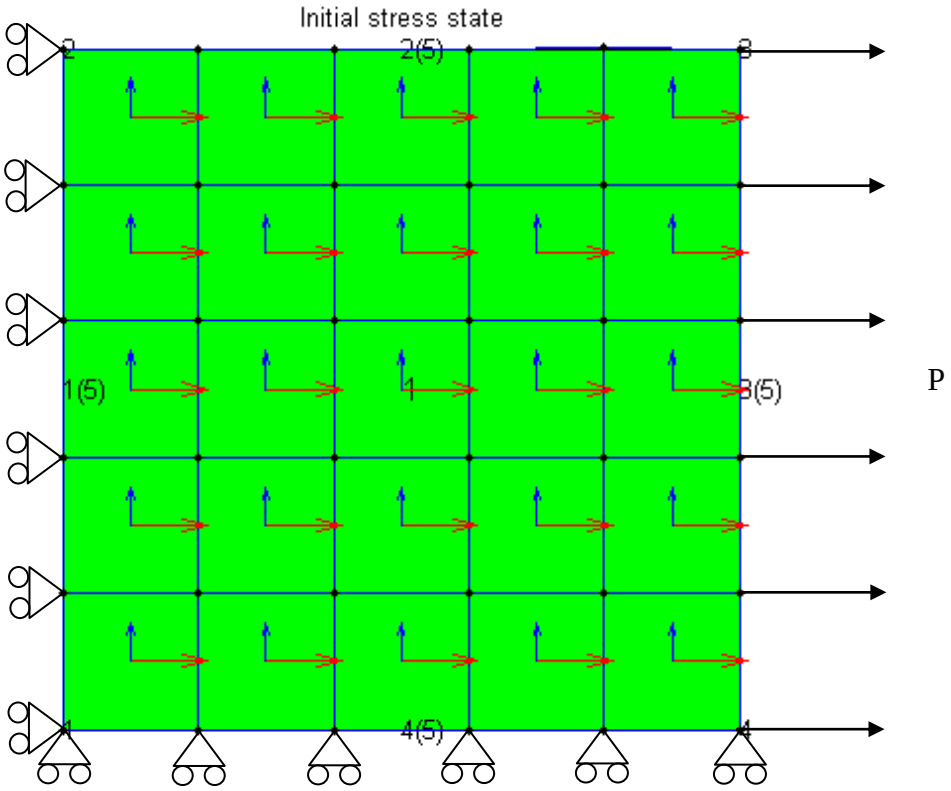

Figure 3.1 Boundary conditions and initial stress state in the plate

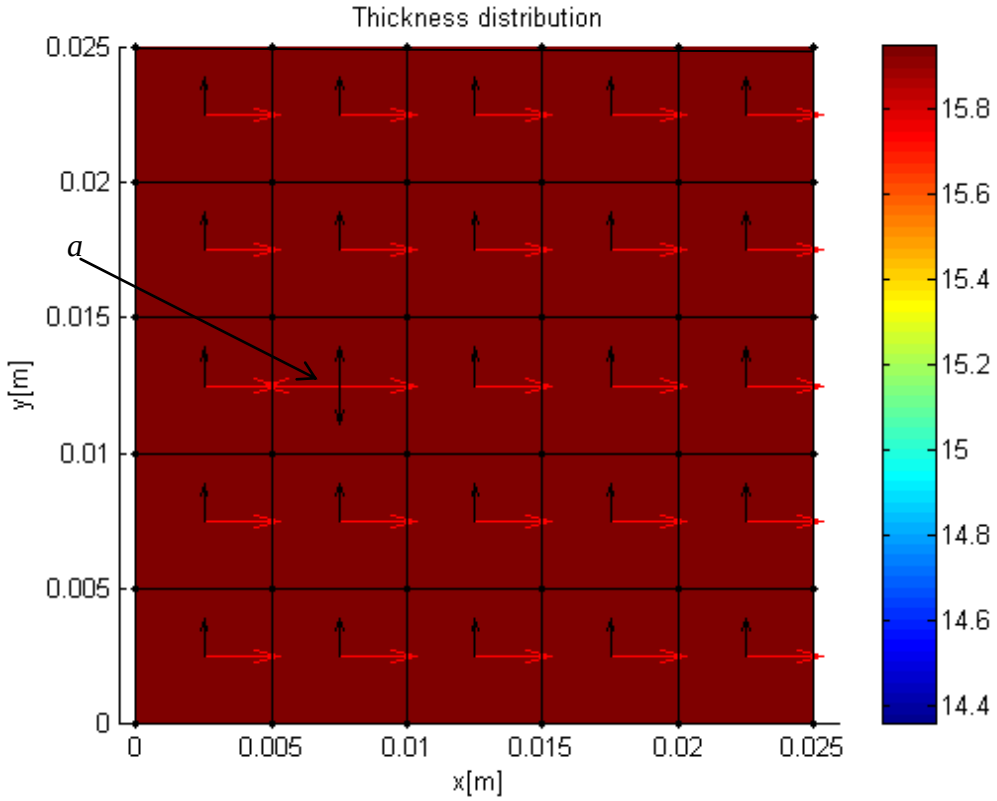

Figure 3.2 Thickness distribution plot for uniaxial tension with a growth factor of 1%.

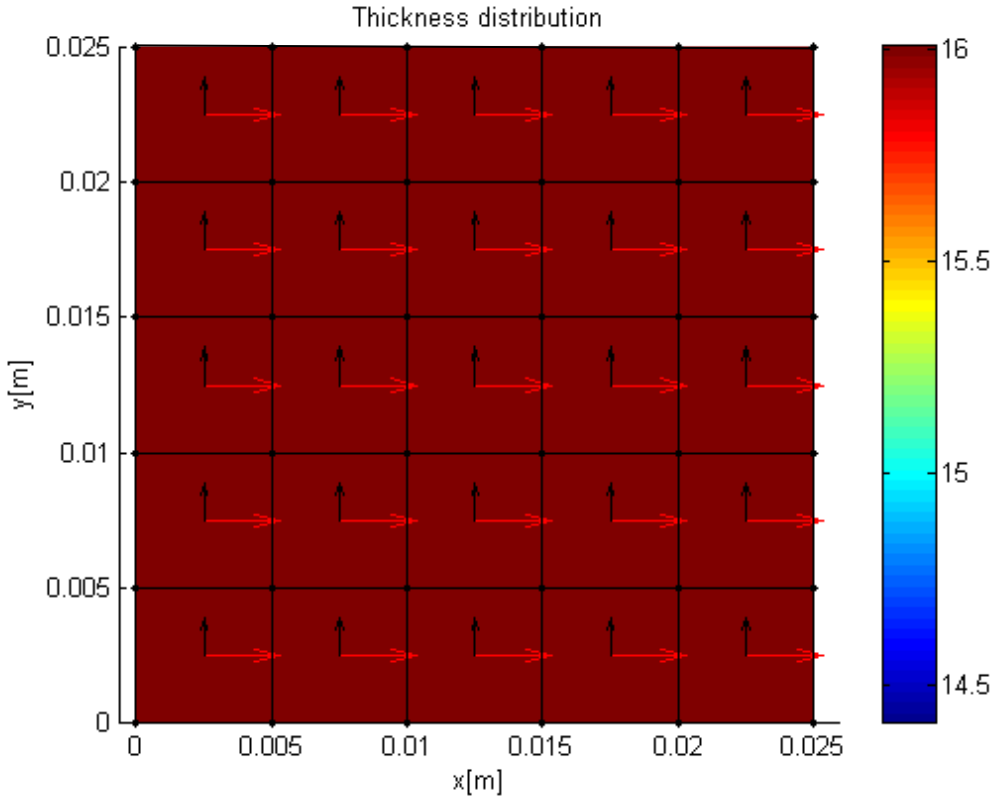

Figure 3.3 Thickness distribution plot for uniaxial compression with a growth factor of 1%.

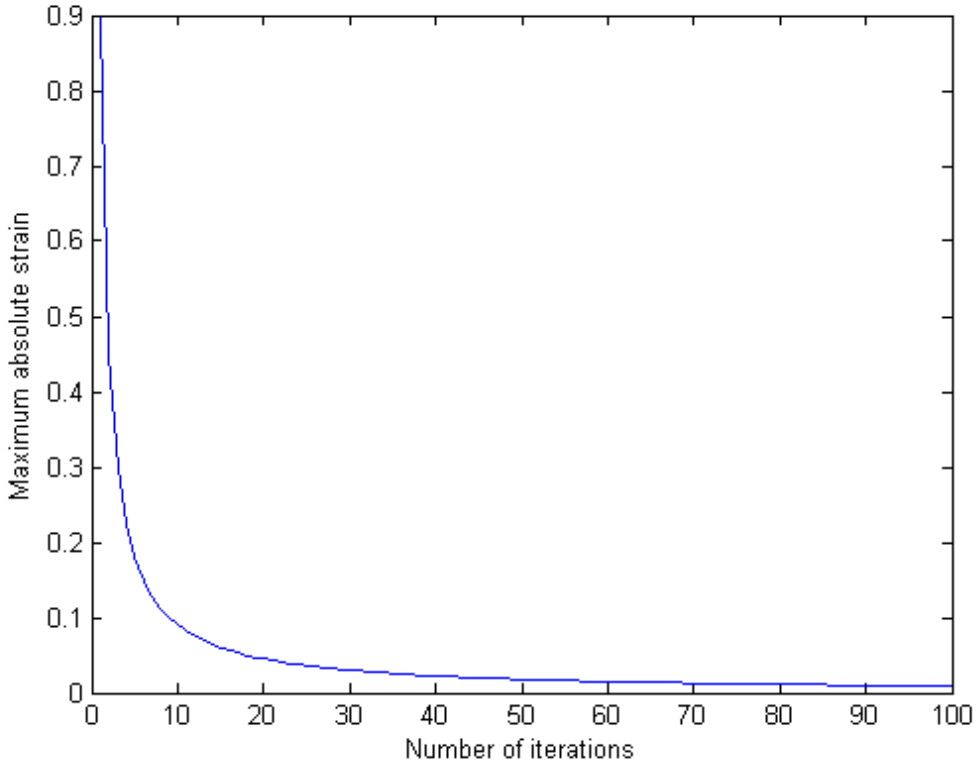

Figure 3.4 Convergence plot for plate under uniaxial tension

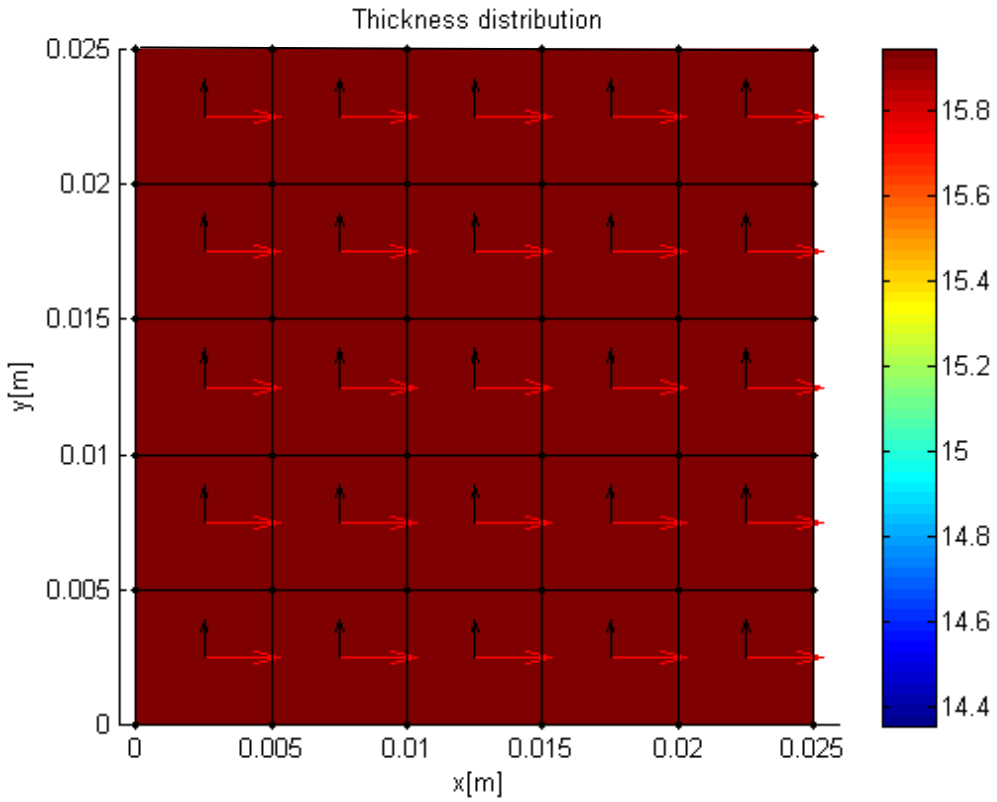

Figure 3.5 Thickness distribution plot for uniaxial tension with a growth factor of 100%.

3.2 Plate under point loading

In this case a vertical point load of 1kN is applied on a 25x25mm square plate at the node on its upper right corner. The analyses are performed for two mesh qualities, one with 25 elements and the other with 100 elements. *Figure 3.5* shows the boundary conditions and initial principal stress state in the isotropic material for coarse mesh. *Table 3.2* shows the number of elements used for the analyses, applied load, the maximum and minimum thicknesses obtained from each analysis, total volume and computation time for both mesh qualities using a slower growth factor in first two analyses and fast growth (100% growth factor) in the third analysis. *Figure 3.7* and *Figure 3.8* show the final thickness distribution for coarser and finer mesh. There are areas marked '*a*' and '*b*' in these figures which will be discussed in the next chapter, Analysis.

Table 3.2 Number of elements, applied load, maximum thickness, minimum thicknesses, total volume and computation time for each calculation for a square plate under point load

Number of elements	Growth factor, η	Load	t_{max} [mm]	t_{min} [mm]	Volume [mm^3]	Computation time [seconds]
25	1%	-1000N	0.48	0.0121	0.12	388
100	1%	-1000N	1.35	0.0011	0.18	2849
100	100%	-1000N	1.40	0.0030	0.19	8

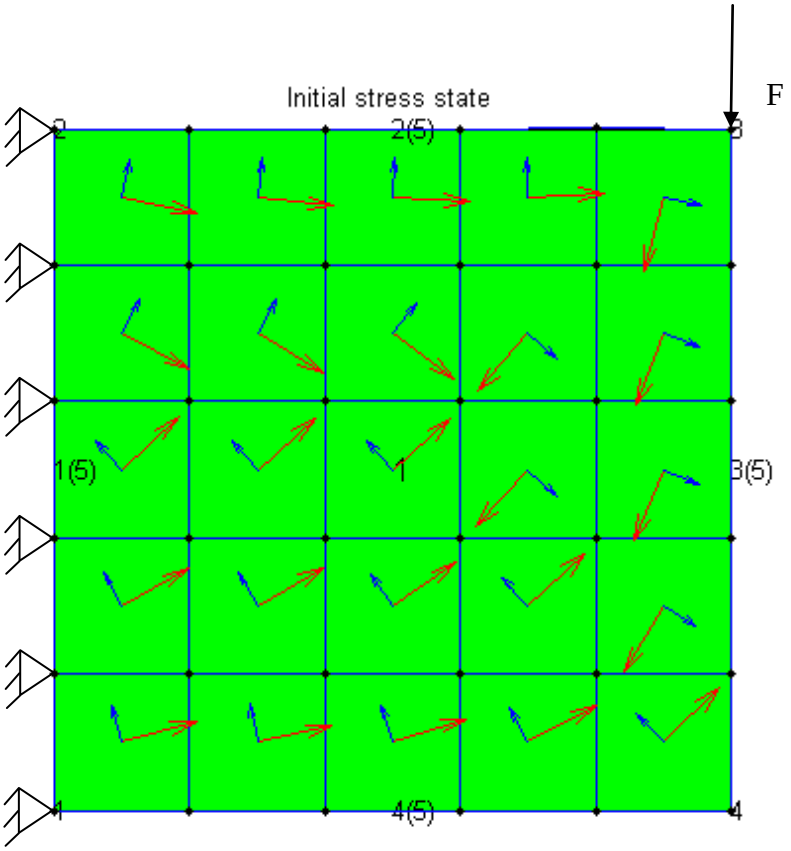

Figure 3.6 Boundary conditions and initial stress state in the plate

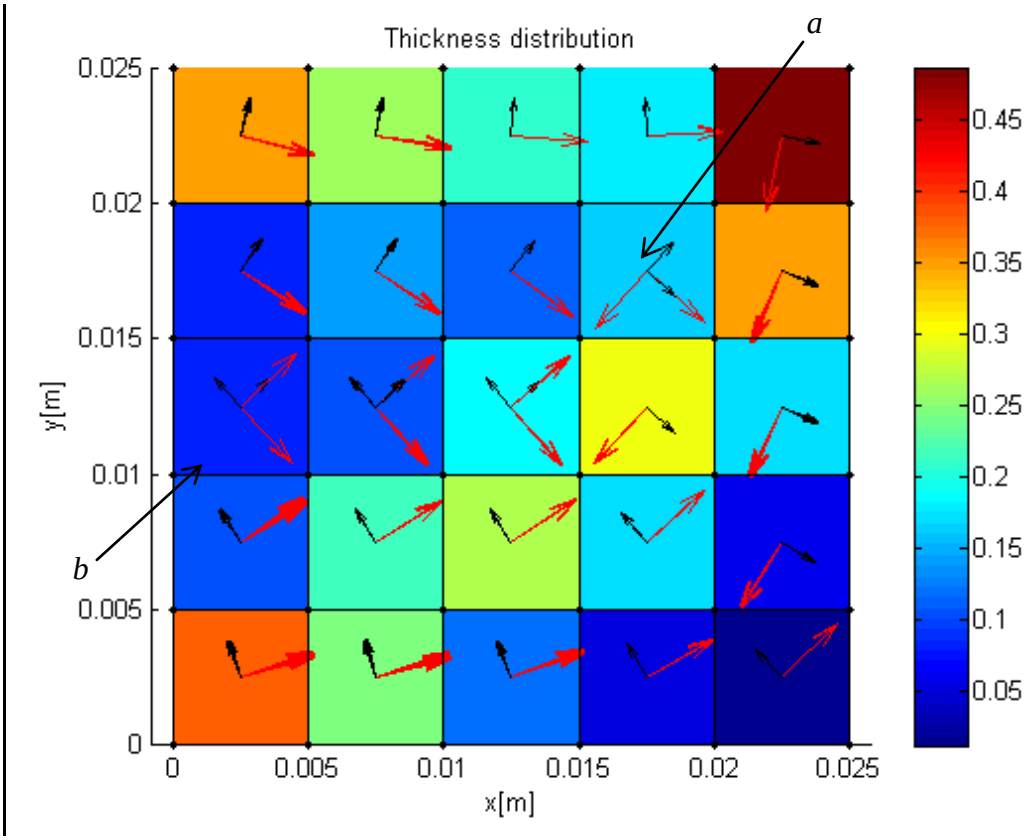

Figure 3.7 *Thickness distribution plot for coarse mesh with a growth factor of 1%.*

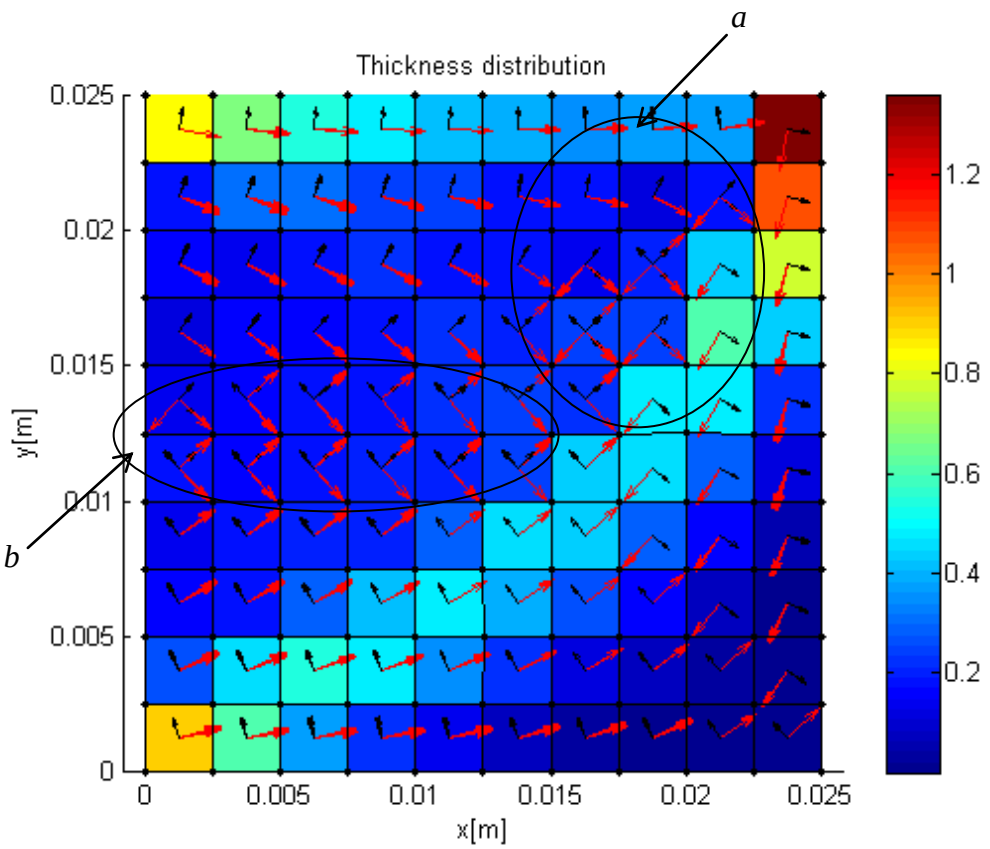

Figure 3.8 *Thickness distribution plot for fine mesh with a growth factor of 1%.*

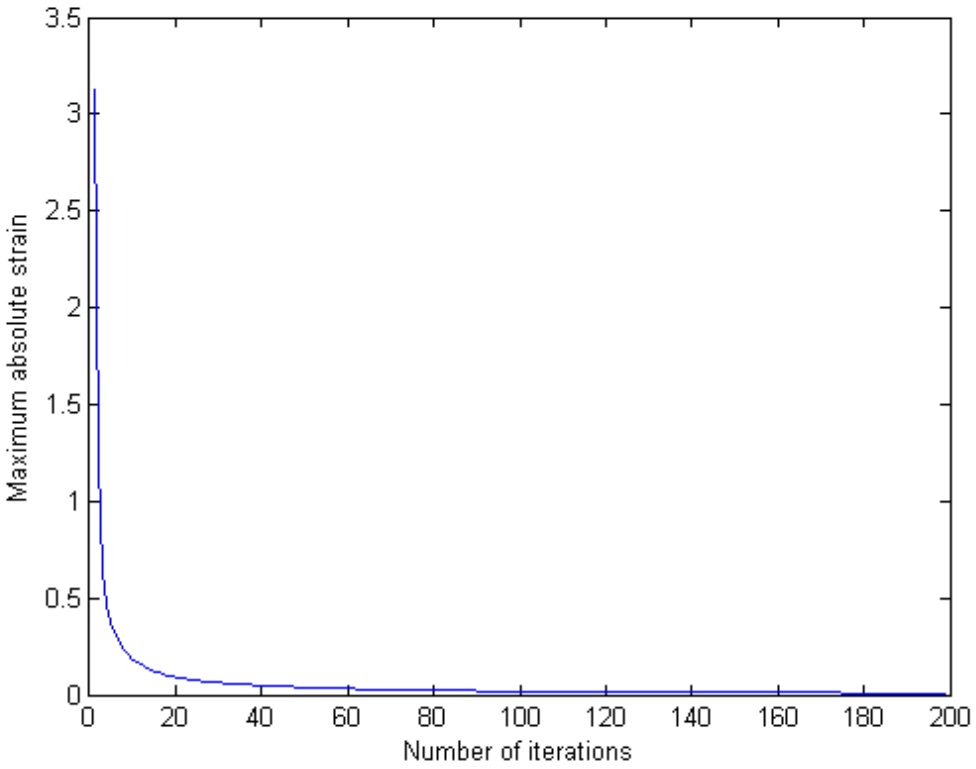

Figure 3.9 Convergence plot for plate under point load with coarse mesh

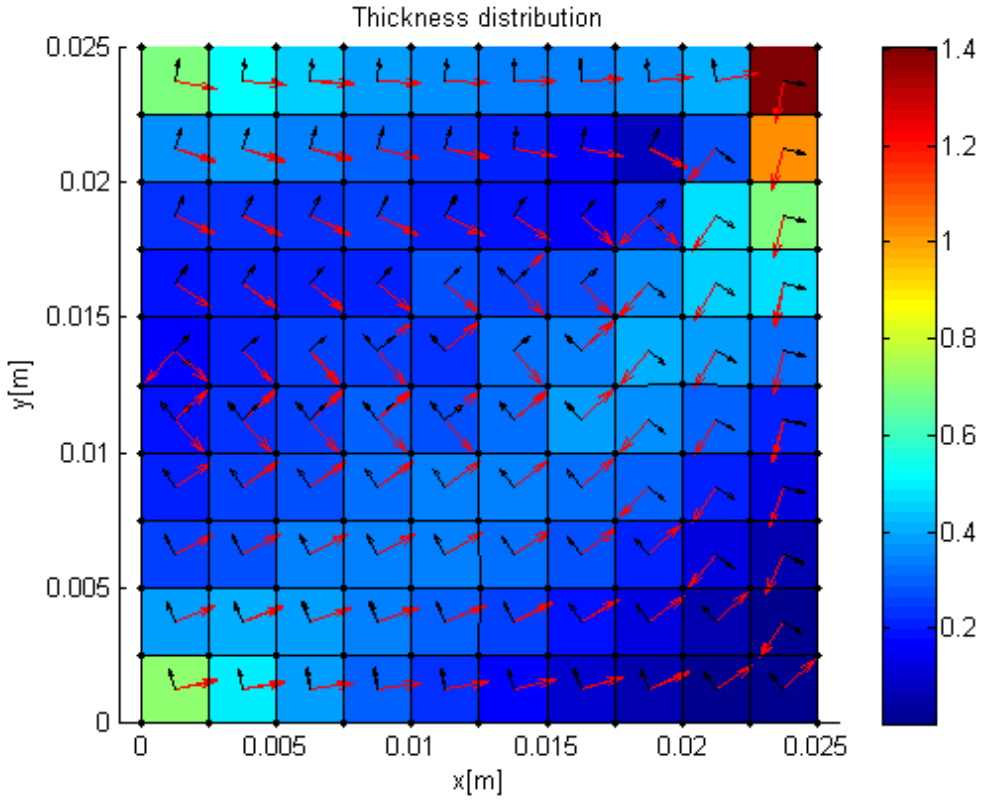

Figure 3.10 Thickness distribution plot for fine mesh with a growth factor of 100%.

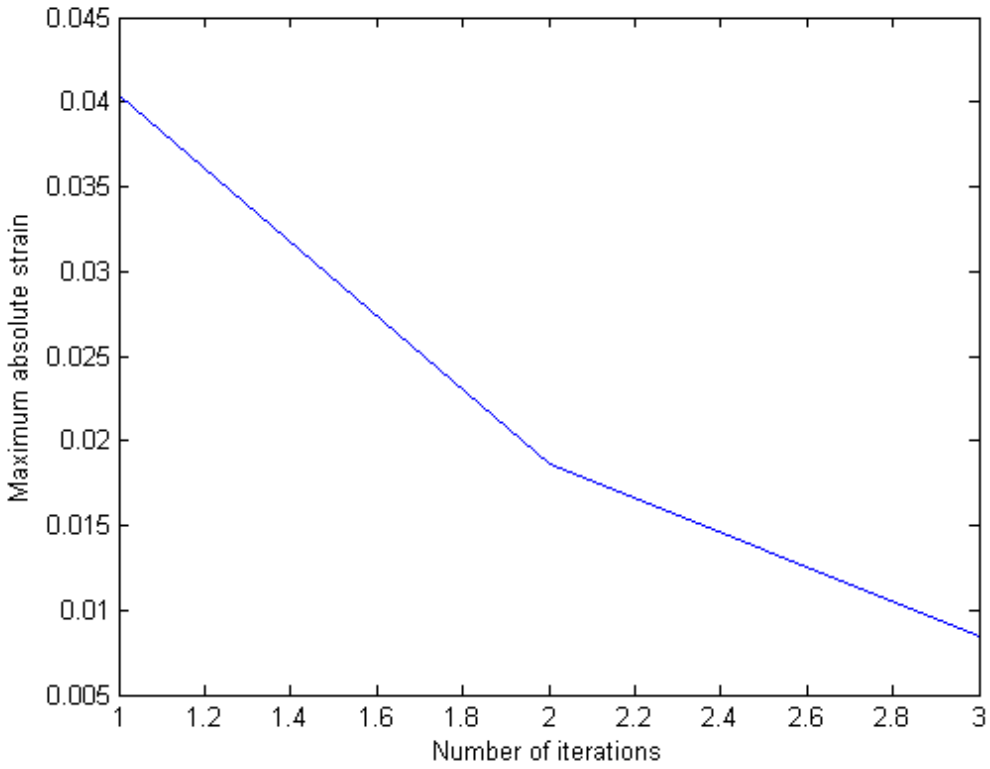

Figure 3.11 Convergence plot for plate under point load with 100% growth factor

3.3 Trapezoid under uniaxial loading

In this case the algorithm is tested on a trapezoidal plate with length of two vertical parallel sides as 40cm and 24cm. The horizontal distance between them is 40cm. Due to symmetry conditions only a quarter of the plate is considered in calculations. *Figure 3.9* shows the symmetry conditions, applied load on the plate and initial principal stress state for isotropic material. A uniform load of 50kN is distributed over the right edge of the plate and the left and bottom sides are constraint in horizontal and vertical directions respectively. Three analyses are performed, i.e. i.)Considering a slow growth factor and a coarse mesh, ii.) Considering a slow growth factor and a fine mesh and iii.) Considering fast growth factor with fine mesh. *Table 3.3* represents the applied load, maximum and minimum thicknesses from each analyses, total volume and computation time required for each analysis.

Table 3.3 Number of elements, applied load, maximum thickness, minimum thicknesses, total volume and computation time for each calculation for a trapezoidal plate under uniaxial tension

Number of elements	Growth factor, η	Load	t_{max} [mm]	t_{min} [mm]	Volume [mm^3]	Computation time [seconds]
25	1%	50000N	0.81	0.19	9.46	124
100	1%	50000N	0.87	0.13	9.80	478
100	100%	50000N	1.61	0.49	17.11	5

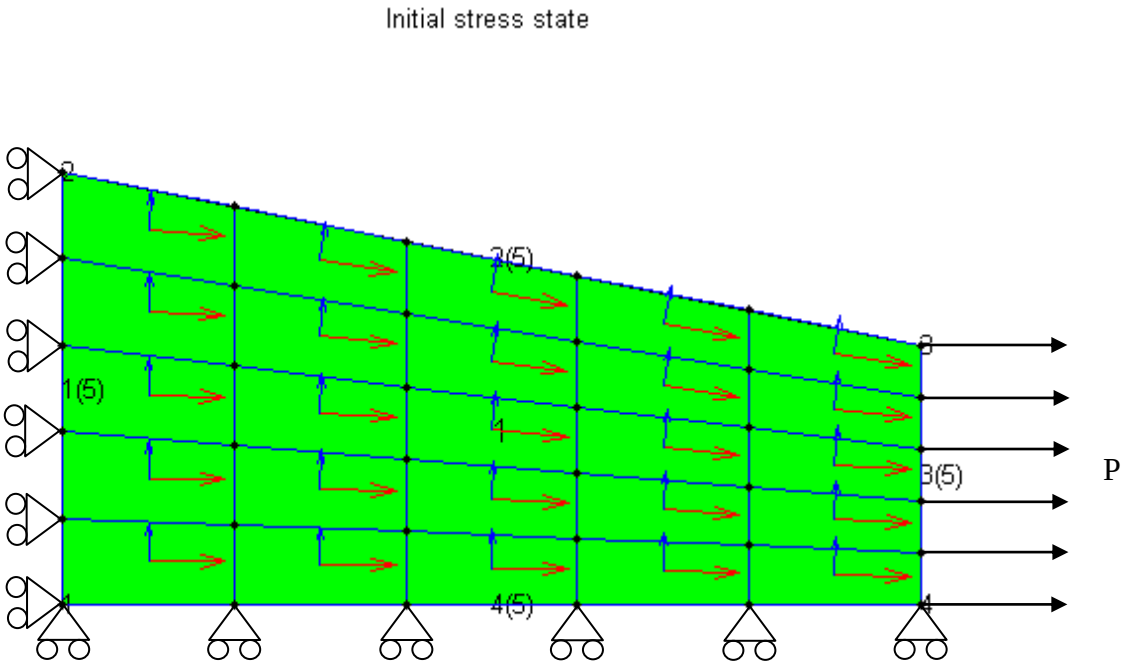

Figure 3.12 Boundary conditions and initial stress state in the plate

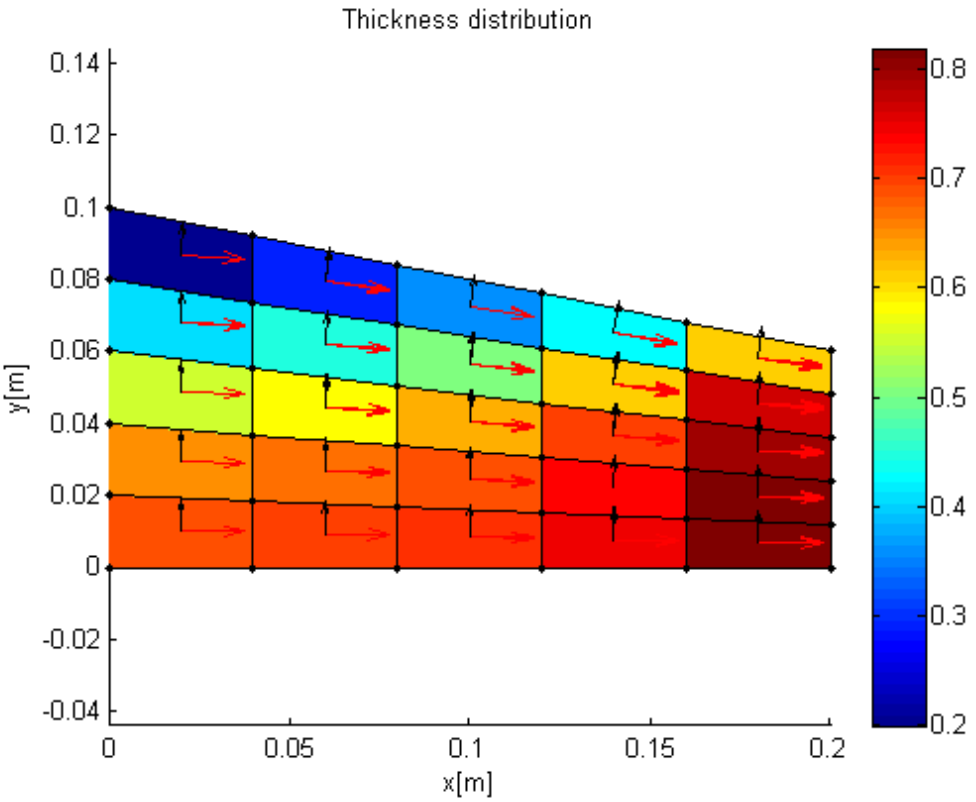

Figure 3.13 Thickness distribution plot for coarse mesh with a growth factor of 1%.

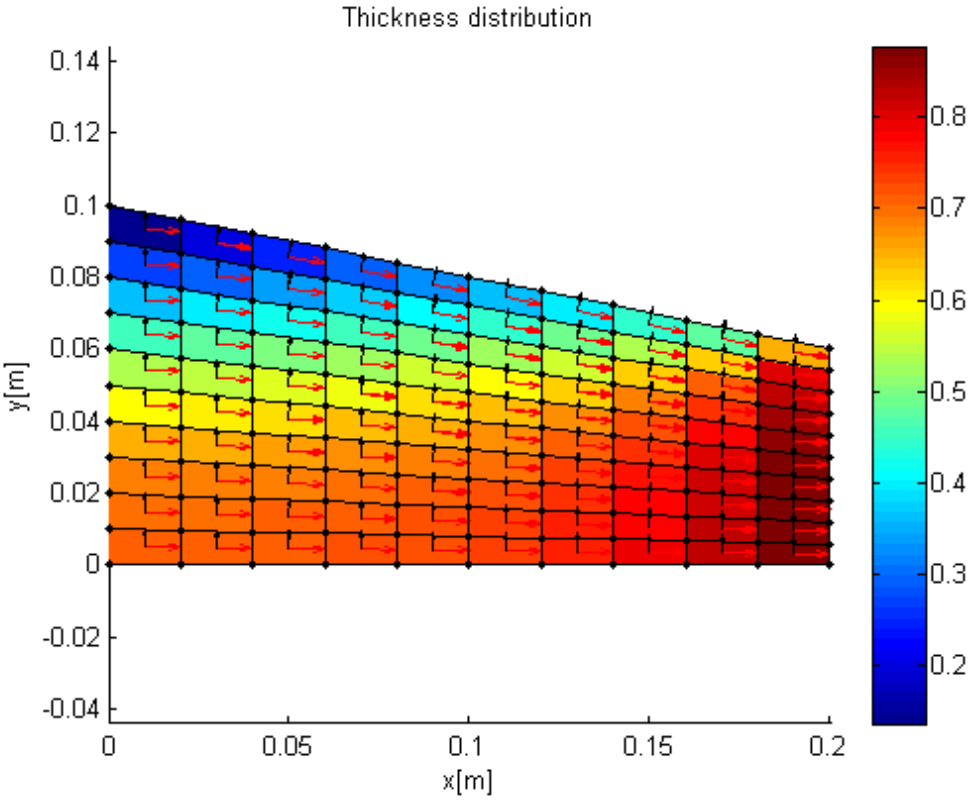

Figure 3.14 Thickness distribution plot for fine mesh with a growth factor of 1%.

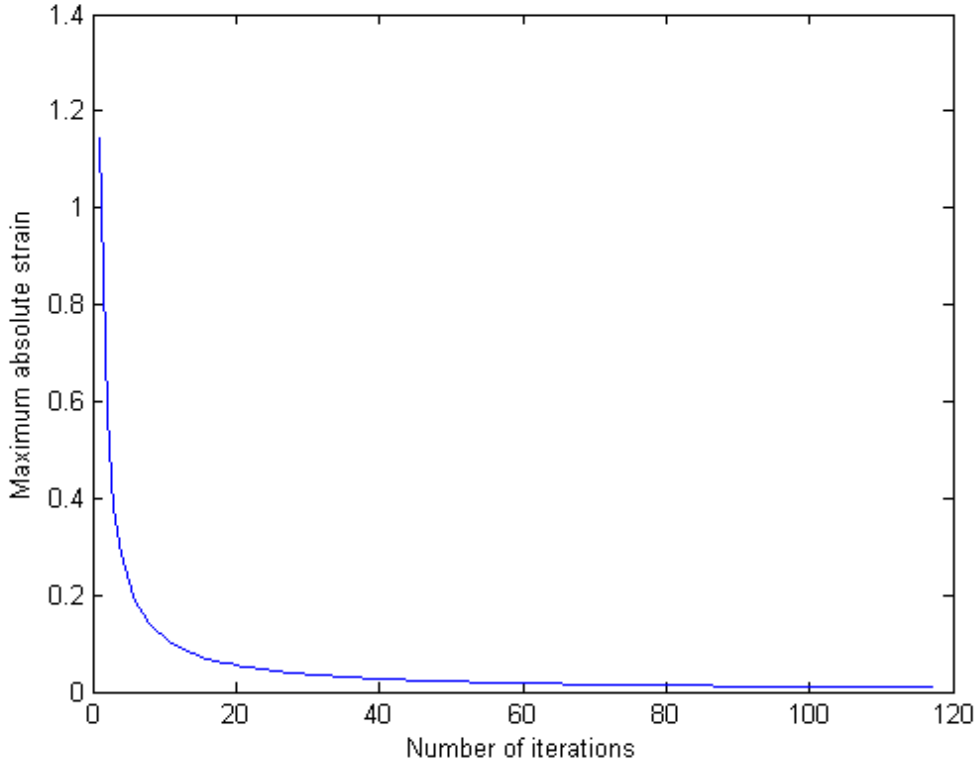

Figure 3.15 Convergence plot for trapezoidal plate under uniaxial load

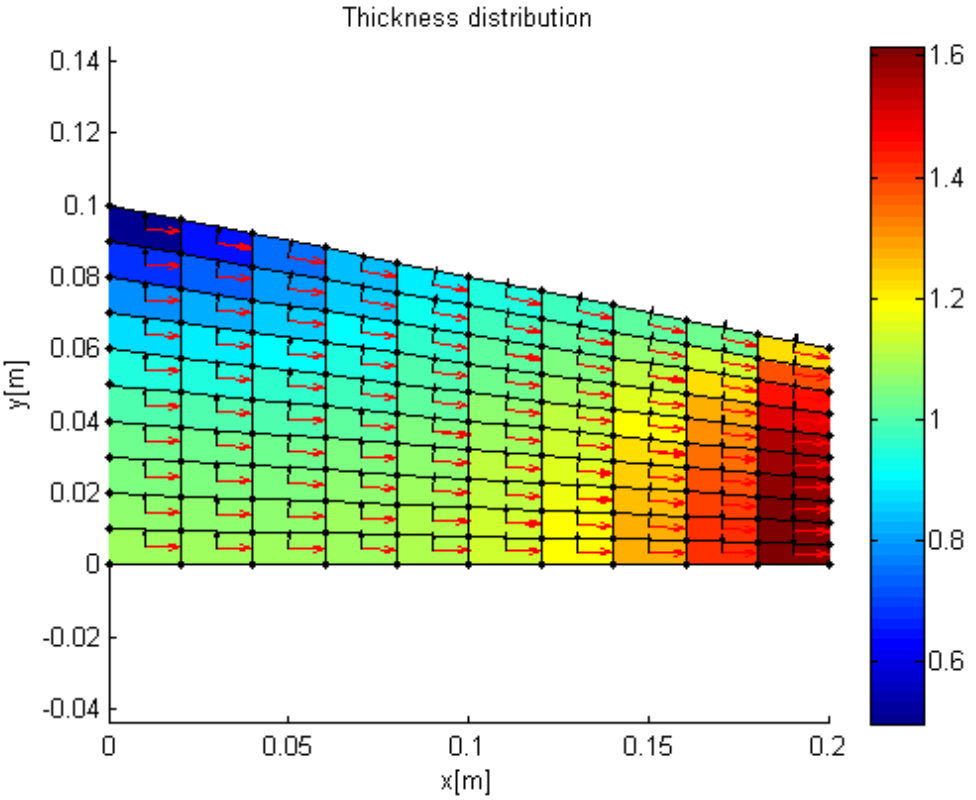

Figure 3.16 Thickness distribution plot for fine mesh with a growth factor of 100%.

3.4 Plate under pure shear loading

In this case the algorithm is tested for a 25x25mm square plate under pure shear. *Figure 3.13* represents the boundary conditions and initial direction of principal stresses. The plate is fixed on left side and shear load of 100kN is applied on rest of the three sides of the plate is such a way that a state of pure shear is obtained. The algorithm is tested for three different conditions similar to those used for earlier cases. The results of the analyses are presented in *Table 3.4*.

Table 3.4 Number of elements, applied load, maximum thickness, minimum thicknesses, total volume and computation time for each calculation for a square plate under pure shear

Number of elements	Growth factor, η	Load	t_{max} [mm]	t_{min} [mm]	Volume [mm^3]	Computation time [seconds]
25	1%	F=100000N	22.22	22.17	13.87	357
100	1%	F=100000N	22.32	22.23	13.91	1220
100	100%	F=100000N	54.27	34.11	26.86	7

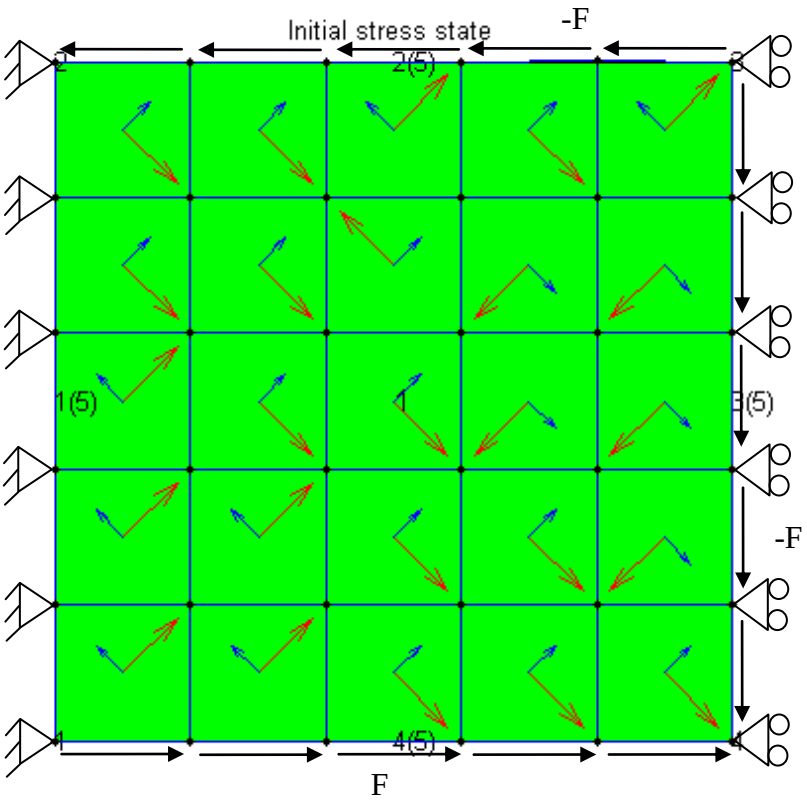

Figure 3.17 Boundary conditions and initial stress state in the plate

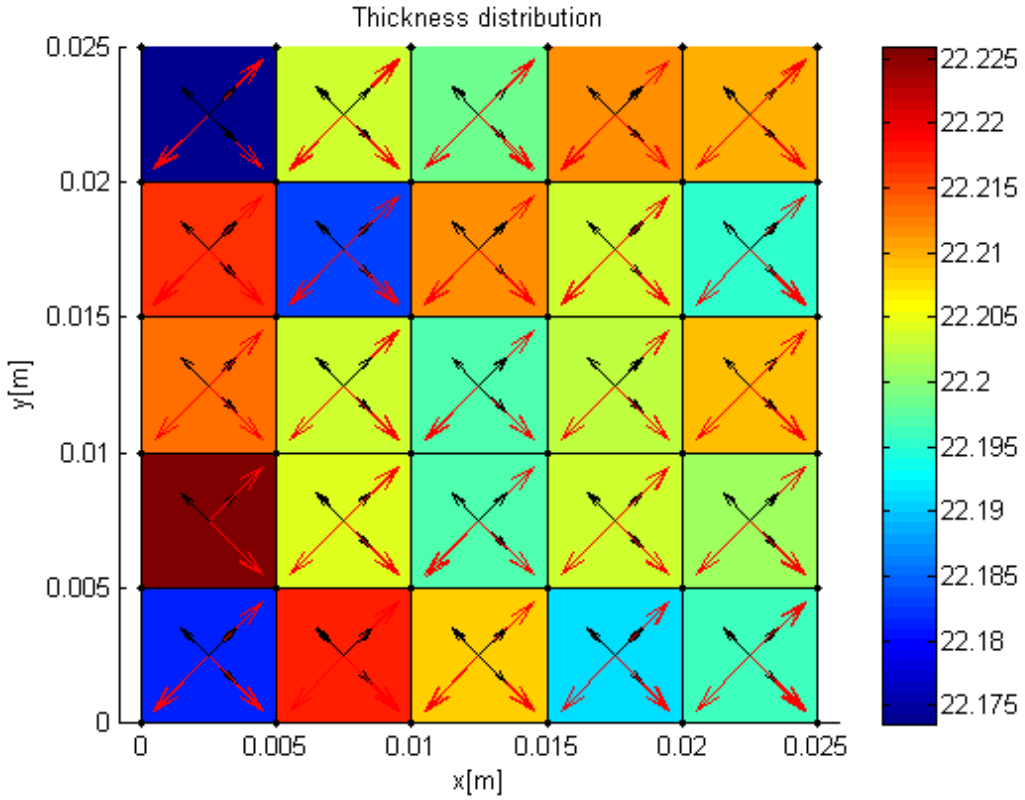

Figure 3.18 Thickness distribution plot for coarse mesh with a growth factor of 1%.

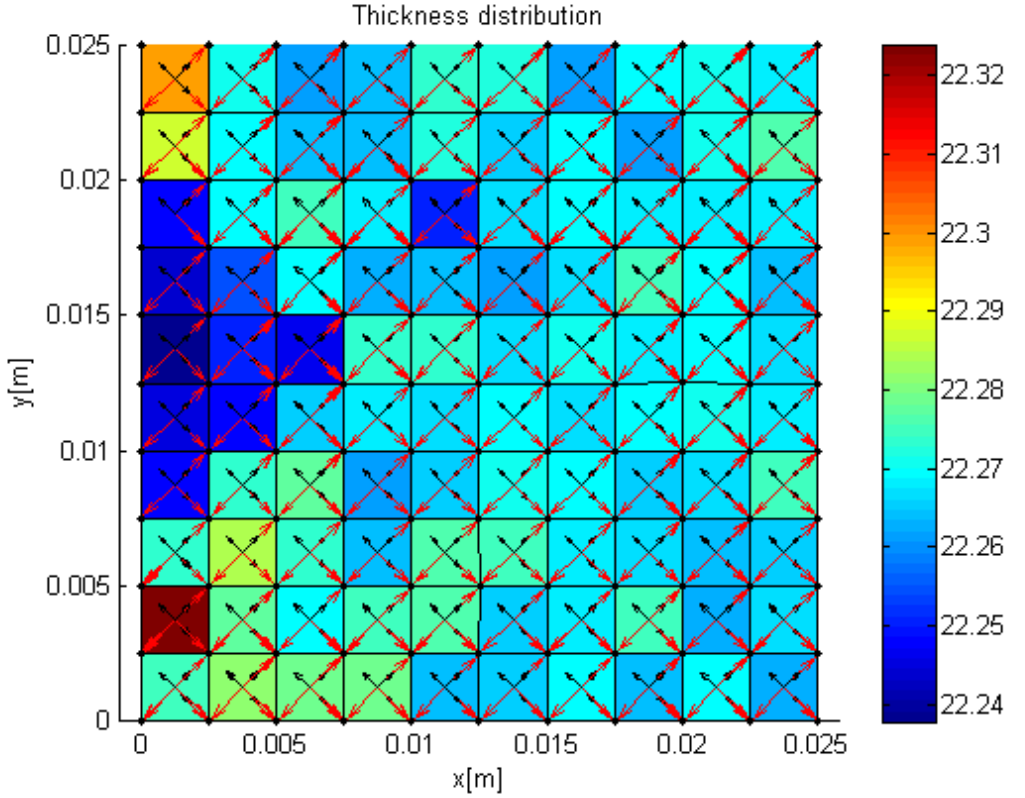

Figure 3.19 Thickness distribution plot for fine mesh with a growth factor of 1%.

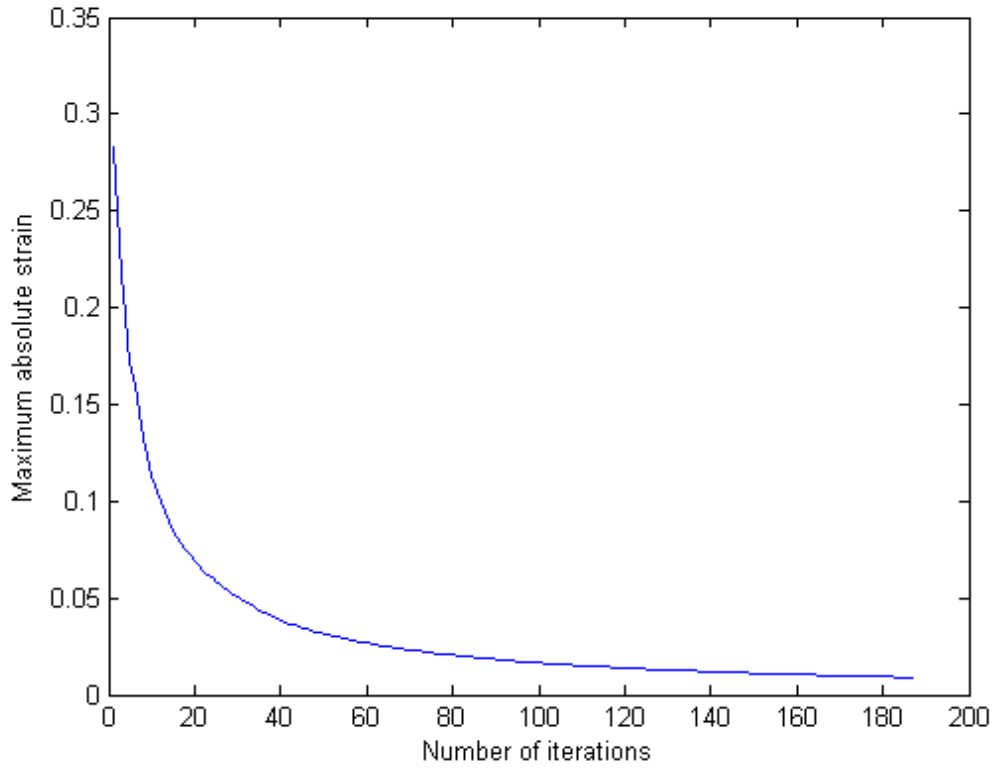

Figure 3.20 Convergence plot for plate under pure shear

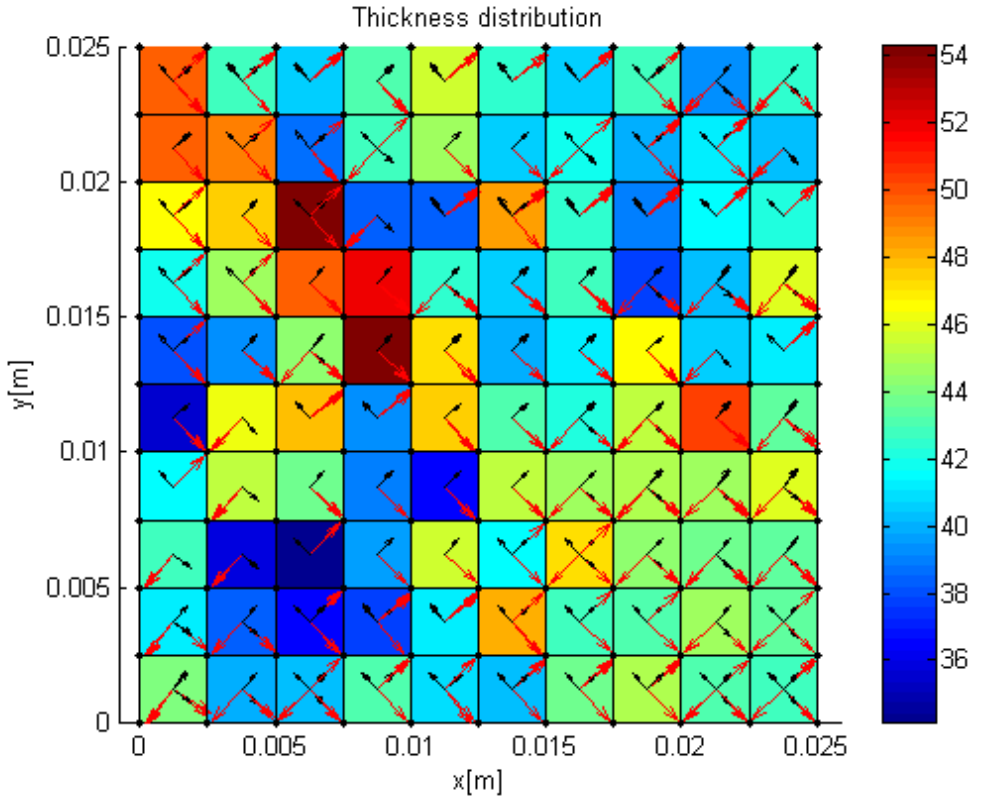

Figure 3.21 Thickness distribution plot for fine mesh with a growth factor of 100%.

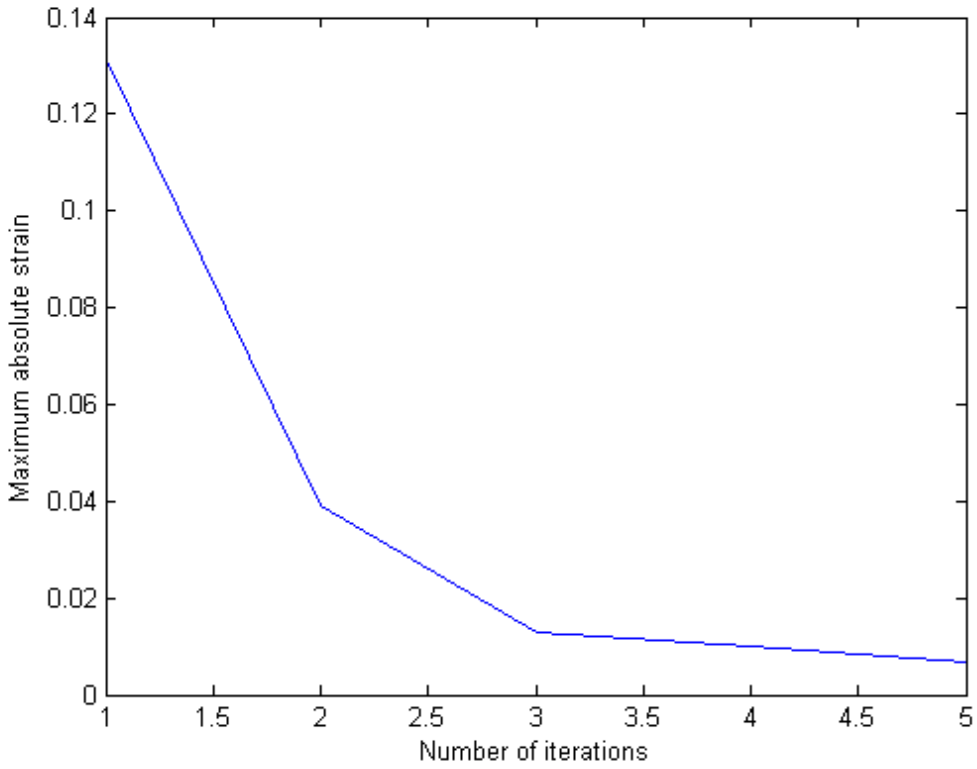

Figure 3.22 Convergence plot for plate under pure shear with 100% growth factor

3.5 Plate with hole under tension

Here the algorithm is used to optimise ply thickness of a 20x20cm plate with a central hole of 10cm diameter. Due to symmetry conditions only a quarter of the plate is considered for calculations. A load of 50kN is applied on the right of the plate, displacement constraints and initial principal stress state for the isotropic material is presented in *Figure 3.17*. Results for coarse and fine mesh with slow growth and fine mesh with fast growth are presented in *Table 3.5*. There are areas marked '*a*', '*b*' and '*c*' in these *Figure 3.24* and *Figure 3.25* which will be Analysed in chapter 4.

Table 3.5 Number of elements, applied load, maximum thickness, minimum thicknesses, total volume and computation time for each calculation for a square plate with a central hole under pure shear

Number of elements	Growth factor, η	Load	t_{max} [mm]	t_{min} [mm]	Volume [mm^3]	Computation time [seconds]
50	1%	50000N	8.72	0.11	11.72	1244
200	1%	50000N	11.82	0.011	15.63	4910
200	100%	50000N	8.51	0.23	18.54	10

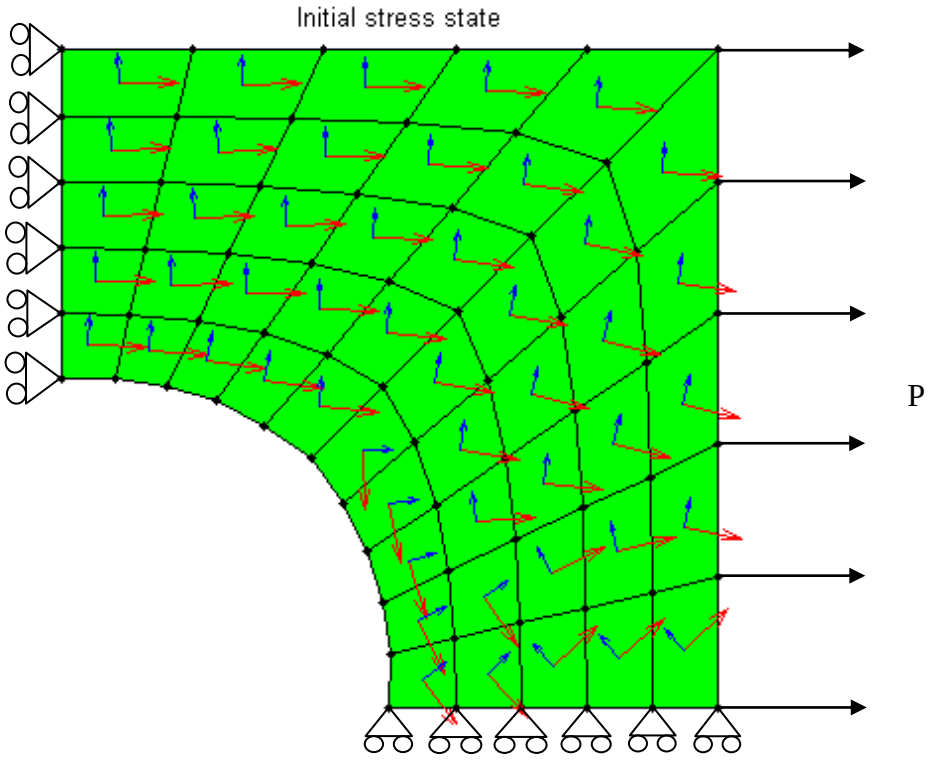

Figure 3.23 Boundary conditions and initial stress state in the plate

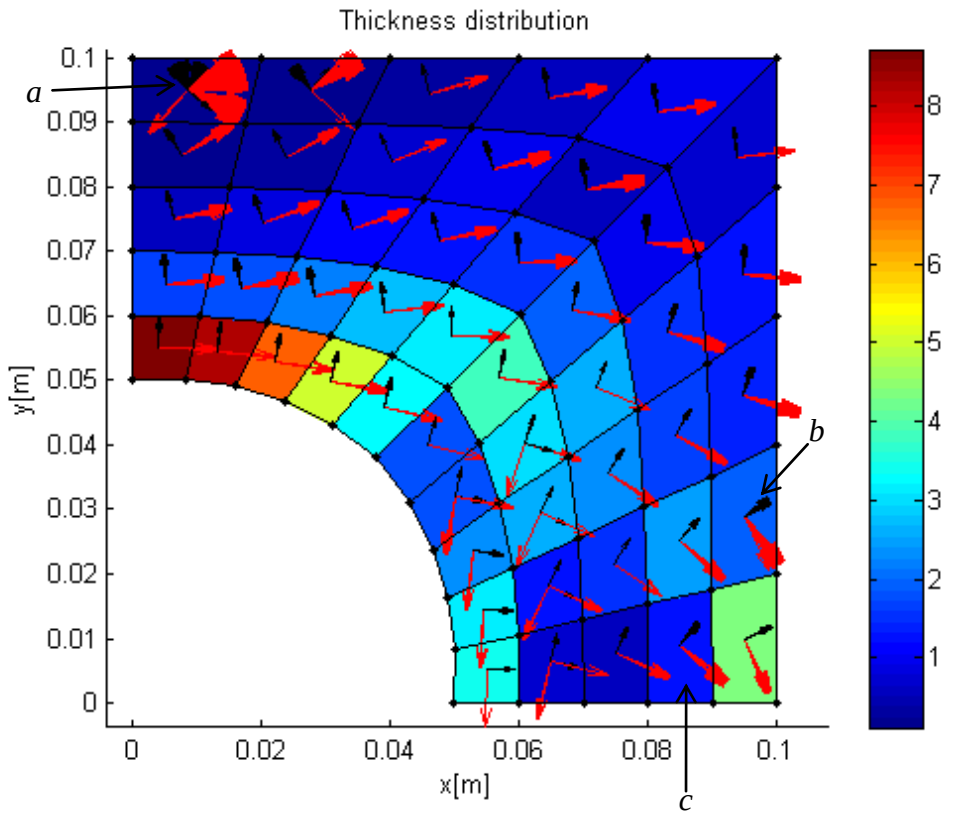

Figure 3.24 Thickness distribution plot for coarse mesh with a growth factor of 1%.

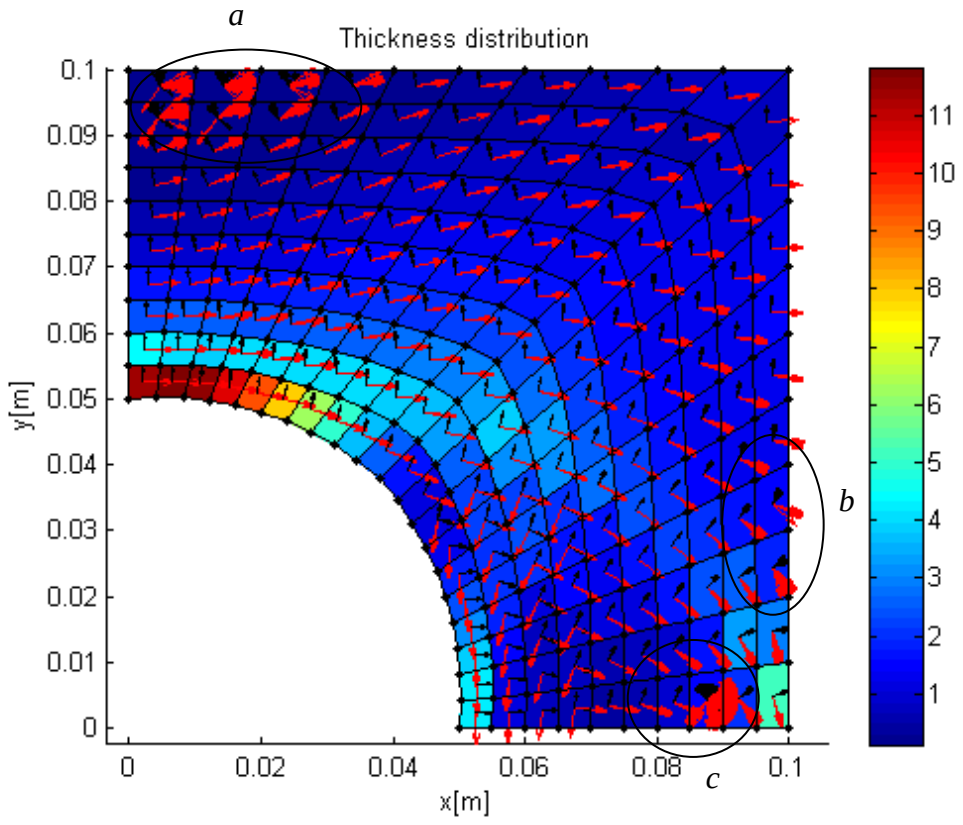

Figure 3.25 Thickness distribution plot for fine mesh with a growth factor of 1%.

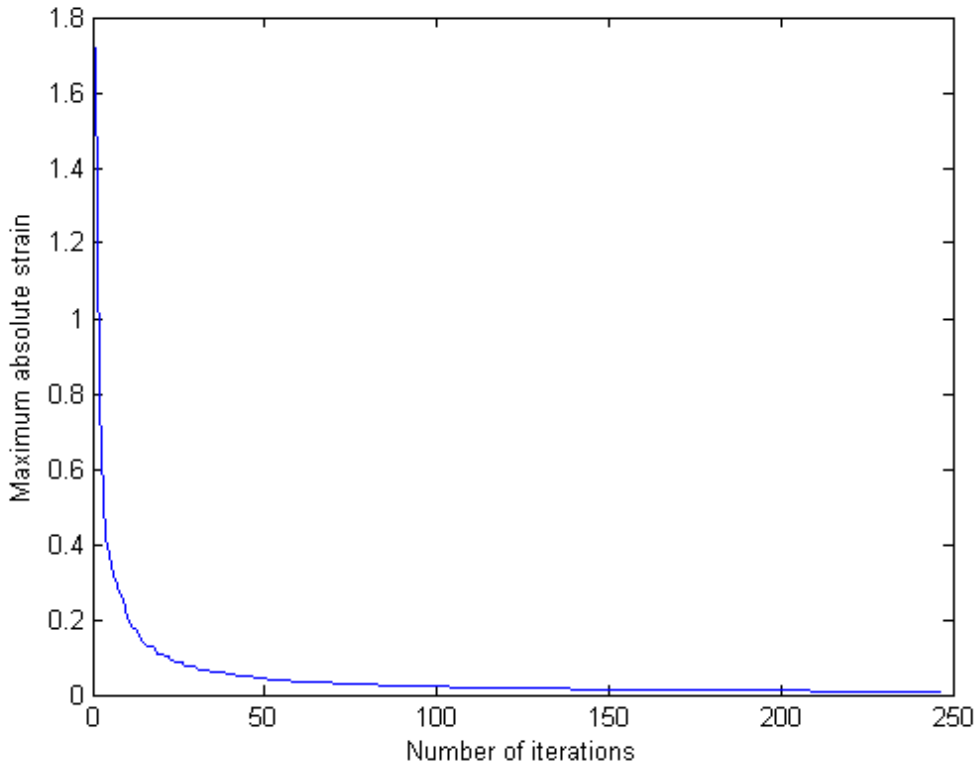

Figure 3.26 Convergence plot for plate with a hole under uniaxial load

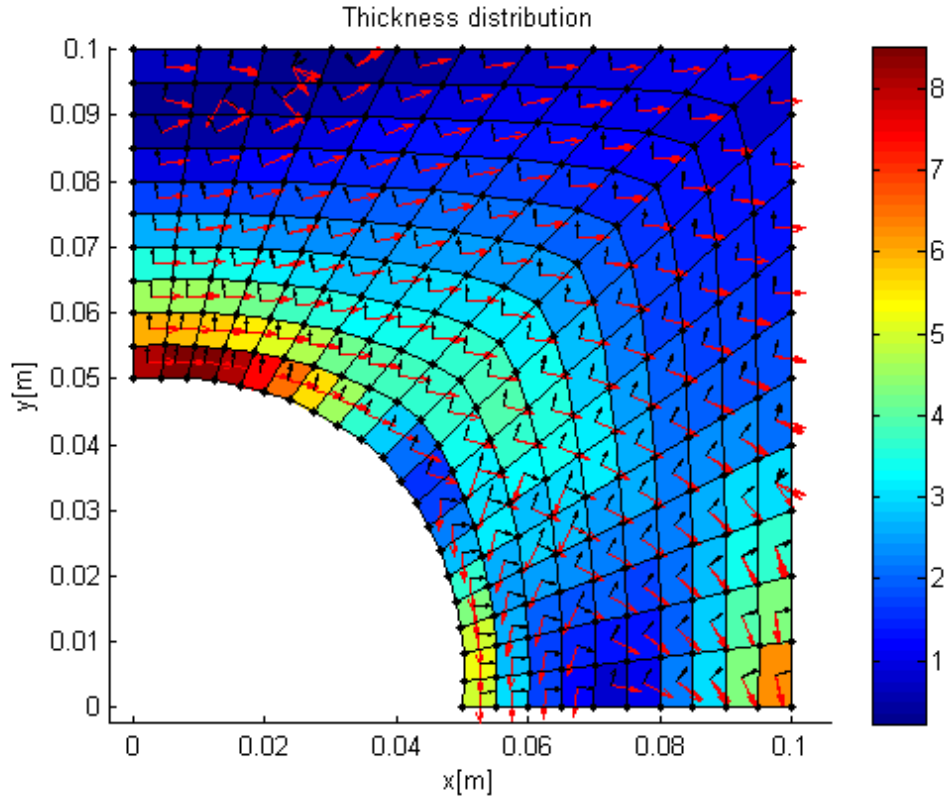

Figure 3.27 Thickness distribution plot for fine mesh with 100% growth factor

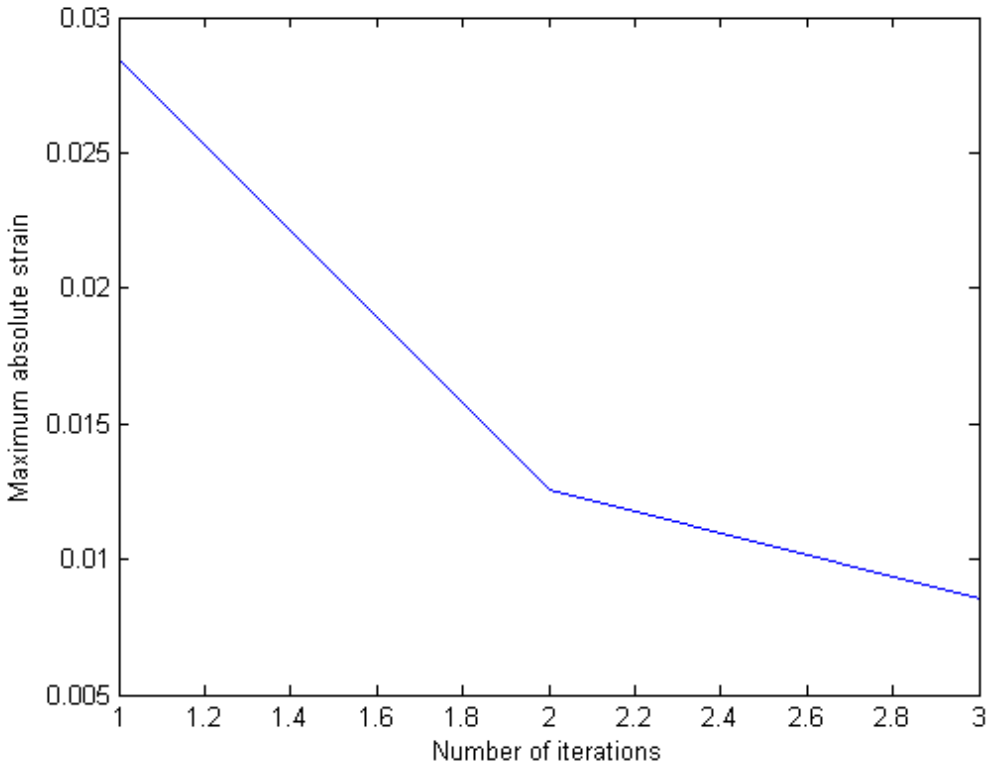

Figure 3.28 Convergence plot for plate with a hole under uniaxial load with 100% growth factor

3.6 Plate under multiple loads

In the last benchmarking problem the algorithm is tested on a 5x5cm square plate under multiple loads. In this case a uniform compressive load of 500kN is applied on the right side of the plate and a point load of 1kN is applied on the upper right node of the plate. The analyses are performed using a coarse mesh with 25 elements and a finer mesh with 100 elements with a small growth factor and 100 elements with 100% growth factor. The boundary conditions and initial state of principal stresses in the isotropic layer is shown in *Figure 3.21*. The results for the three analyses are presented in *Table 3.6*.

Table 3.6 Number of elements, applied load, maximum thickness, minimum thicknesses, total volume and computation time for each calculation for a square plate under mixed load

Number of elements	Growth factor, η	Load	t_{max} [mm]	t_{min} [mm]	Volume [mm^3]	Computation time [seconds]
25	1%	F= -1000N P= -500000N	16.29	15.74	10.02	101
100	1%	F= -1000N P= -500000N	16.70	15.711	10.13	357
100	100%	F= -1000N P= -500000N	16.99	16.56	10.44	4

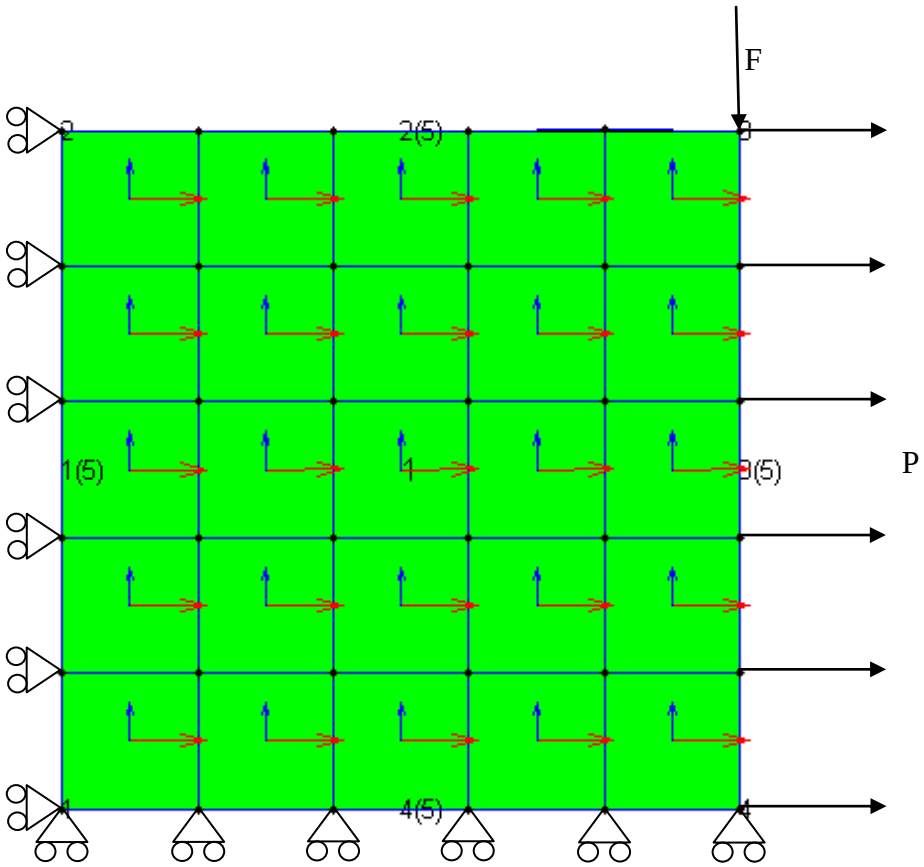

Figure 3.29 Boundary conditions and initial stress state in the plate

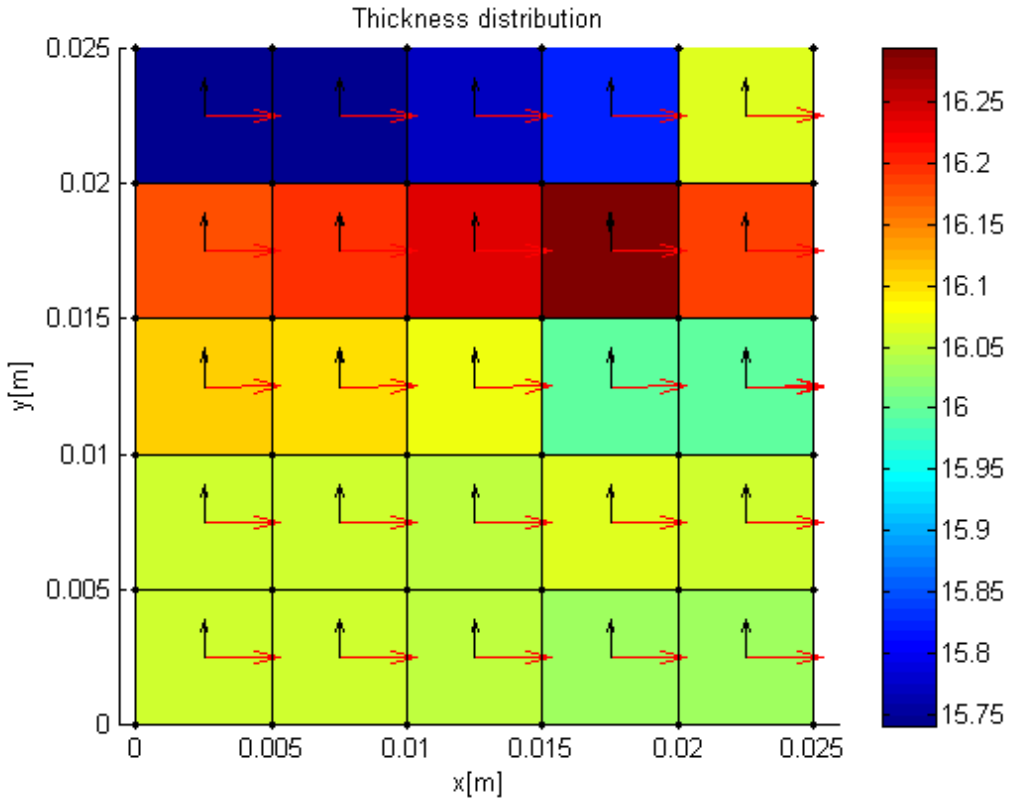

Figure 3.30 Thickness distribution plot for coarse mesh with a growth factor of 1%.

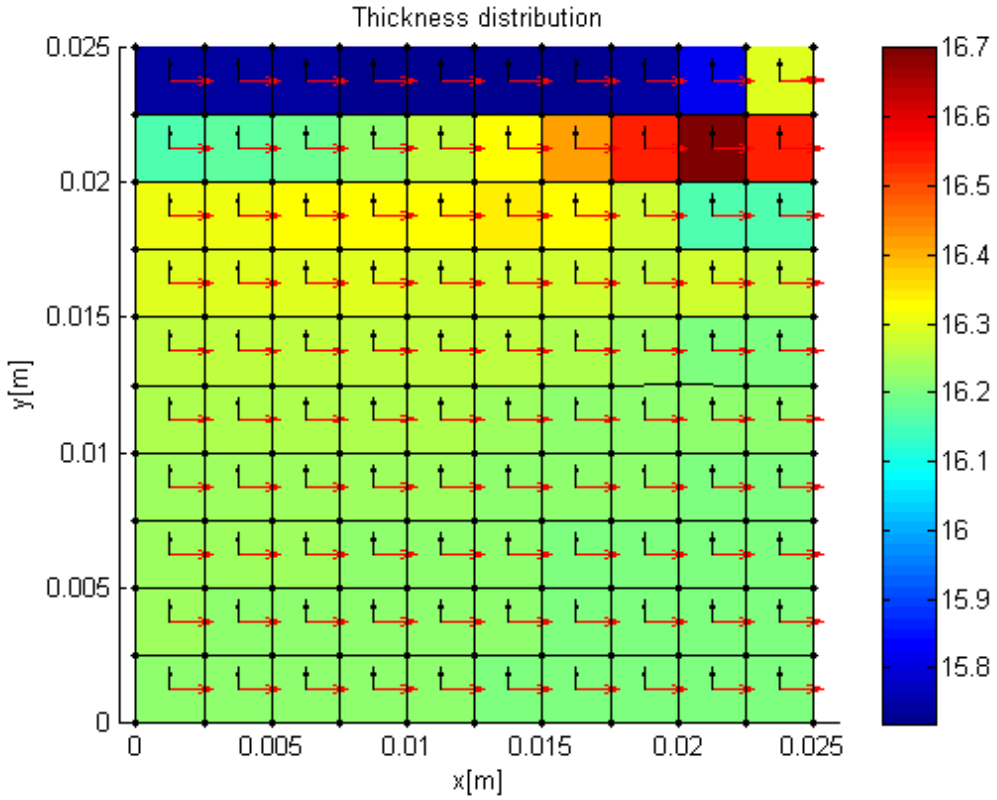

Figure 3.31 Thickness distribution plot for fine mesh with a growth factor of 1%.

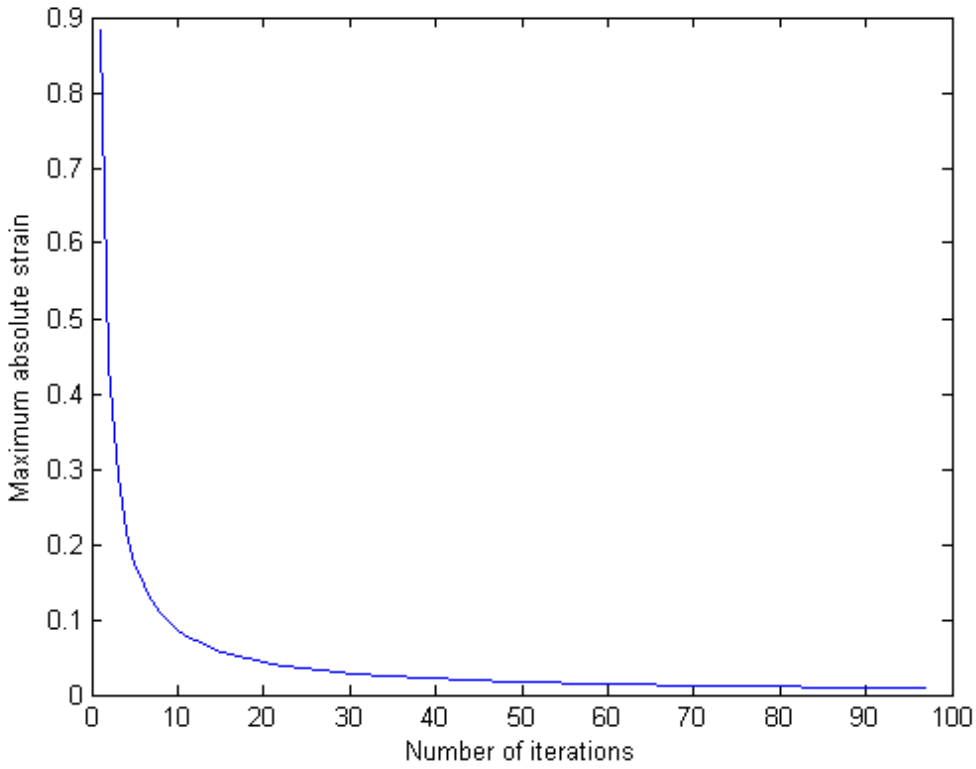

Figure 3.32 Convergence plot for plate under mixed loading

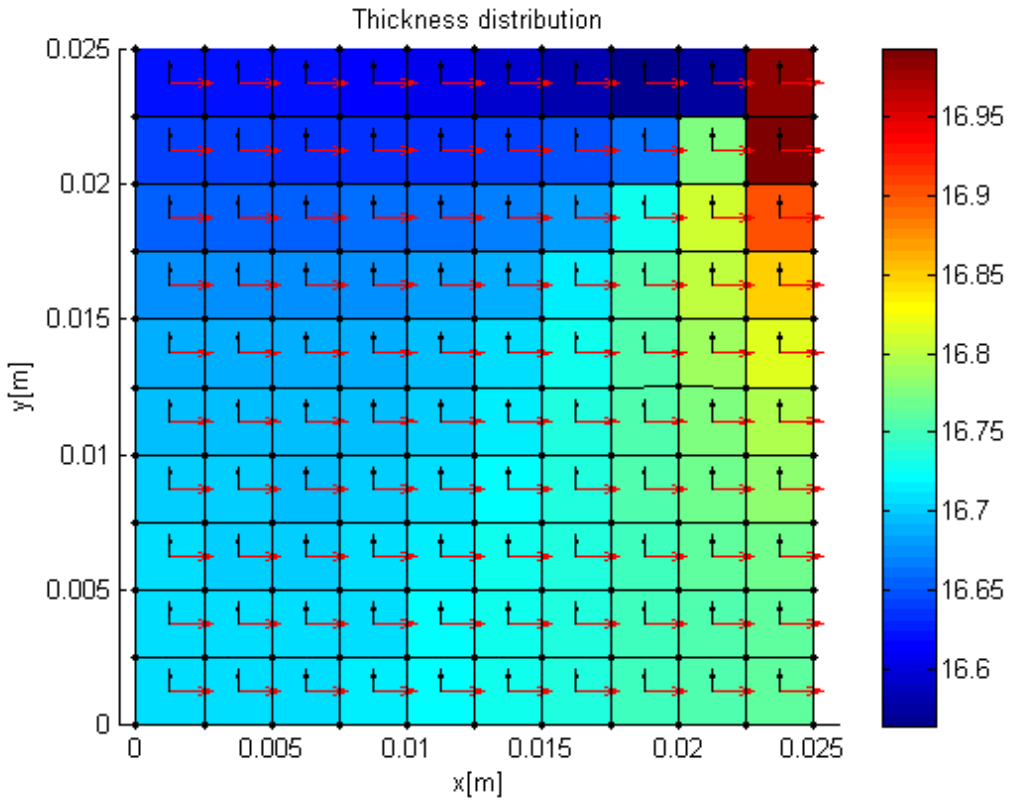

Figure 3.33 Thickness distribution plot for fine mesh with a growth factor of 100%.

4 Analysis

In the first case study a 10x10cm square plate is loaded with uniaxial tensile force. Due to symmetry conditions, only a quarter of the plate is considered for analysis as shown in *Figure 3.1*. The initial principal stress orientation is also shown in this figure. For this case the main principal stress is at 0^o and the second principal stress equals zero for all the elements. As a consequence all the fibres are orientated along the main stress direction and the thickness of all the elements is equal due to homogeneous stress state in the plate, *Figure 3.2*. In elements marked as *a*, a rotation of 180^o could be observed which due to numerical scatter that come while calculating the principal stress direction. It should be noted that the vectors inside the elements in *Figure 3.1* and *Figure 3.2* represent the orientation of principal stresses and not their directions. The results for this case are verified analytically as follows:

$$allowable\ stress\ in\ first\ principal\ direction = \sigma_{max} = 0.6 * \sigma_{1f}.$$

As it is known for the uniaxial case, stresses in the second principal direction are zero and the strain in this direction is not considered in calculations. So,

$$\sigma_1 = \sigma_{max} = \frac{F}{lt} \Rightarrow t = \frac{F}{l\sigma_{max}},$$

$$t = 0.0161m.$$

There is a minor difference in between the analytical and computational result. It is due to the fact that the stiffness of the isotropic layer is ignored in calculation of the stiffness which slightly changes the elements of $[Q]$ matrix. The maximum allowable strain for composite strength, σ_{max}, and stiffness in axial direction, E_{11}, the allowable strain is 0.88% which is rounded off to 0.9% in the algorithm. The algorithm is also evaluated for optimisation of the thickness using a 100% growth factor. It takes one ply increment loop to converge and the thickness distribution is shown in *Figure 3.5*. In the case of faster growth it is observed that the thickness is equal to the case when slow growth factor is employed to optimise the plate thickness.

In case of unaxial compression, the direction of the main principal stress is the same but with opposite sign. Like for the uniaxial tensile loading, fibres are aligned in the main direction only. Since the composite strength is lower in compression than in tension, the elements are thicker in this case than for the case of unaxial tension for the same load as shown in *Figure 3.3*. As the stress state inside the plate is

homogeneous for uniaxial tension and compression, increasing the number of elements will not affect the results.

In the second case studied here, a point load is applied at one of the nodes to represent a cantilever loading. The boundary conditions and initial principal stresses orientation is shown in *Figure 3.6*. *Figure 3.7* shows the total thickness distribution, that is thickness due plies in main principal stress as well as plies in second fibre direction, for a coarser mesh of 25 elements. The result for a finer mesh with 100 elements is shown in *Figure 3.8*. As could be expected, thickness distribution is more refined in this case. A region of thicker elements forming a shape of a '7' can be noticed in this figure. It is also shown in *Figure 3.7* and *Figure 3.8* that there are elements, marked as *a* and *b*, in which the principal stresses rotate by 90^o. These elements are either in the vicinity of highly loaded elements or in the regions where the strains decrease very rapidly when the thickness of highly strained elements increases. The convergence for both coarse and fine mesh is obtained in 198 and 297 iterations respectively and the convergence plot for the case of coarser mesh is shown in *Figure 3.9*. The algorithm is then used to optimise the plate thickness using 100% growth factor. The result of thickness distribution and convergence are shown in *Figure 3.10* and *Figure 3.11*. On comparison between *Figure 3.8* and *Figure 3.10* it is observed that smaller growth factor gives well defined difference in thickness between highly stressed regions than compared to the higher growth factor.

The third case is the application of uniaxial load on a trapezoidal plate. Due to symmetry conditions, one quarter of the plate is considered for calculations. Since a constant pressure is applied on smaller side of the trapezoid, the elements near the centre of the shorter side are thicker than the rest of the plate as they undergo maximum strain. This is evident from analyses using both coarse and fine mesh of the plate as shown in the total thickness plot of *Figure 3.13* and *Figure 3.14*, respectively. The plot representing maximum absolute strain versus number of iterations is shown in *Figure 3.15*. As for previous cases the algorithm is then used to optimise the plate thickness using 100% growth factor and its result of thickness distribution is shown in *Figure 3.16*. For this case it takes one iteration loop to convergence when the growth factor is 100%.

Next the algorithm is tested for the case of a plate under pure shear. The boundary conditions and the initial principal stress state are shown in *Figure 3.17*. In this case both principal stresses will be equal and oriented at $+45^o$ and -45^o from the

x-axis respectively. Therefore the plies thickness in both directions should be equal. In an ideal situation the thickness plot should have shown uniform thickness distribution as the stress-strain state in the plate is homogeneous. But due to shear locking effect of lower order 4-node quadrilateral element difference in element thickness is obtained as shown in *Figure 3.18* and *Figure 3.19*; See also Section 1.4. The decrease in maximum absolute strain with increasing ply thickness is shown in *Figure 3.20*. As for previous cases the algorithm is then used to optimise the plate thickness using 100% growth factor and its results of thickness distribution and convergence are shown in *Figure 3.21* and *Figure 3.22*.

In the next step the algorithm is used to optimise the ply thickness of a plate with a hole in its centre. Thickness distribution for fine and coarse meshes is shown in *Figure 3.24* and *Figure 3.25* respectively. As could be seen in the encircled regions in *Figure 3.24* and *Figure 3.25*, there are elements where the principal stresses change their directions very abruptly. These elements are in regions with very low stress and the stress here decrease rapidly when thickness of the highly stressed elements nearby increases. However, the main stress direction in the highly stressed elements does change the direction. Decrease of maximum absolute strain with every iteration is shown in *Figure 3.26*. Results for the case of 100% growth factor are shown in *Figure 3.27* and *Figure 3.28*. As could be seen from *Figure 3.25* and *Figure 3.27*, the result of slower growth rate shows distinct region of minimum thickness such as regions *a, b* and *c* in *Figure 3.25*. However in case of higher growth factor the thickness distribution in *Figure 3.27* shows a higher material density in the same places as regions *a, b* and *c*.

The last case for which the algorithm is benchmarked is a case of mixed load where a vertical point load acts at the top right node and a uniaxial compressive load is applied on the right side of the plate as shown in *Figure 3.29*. The results for thickness distribution for coarse and fine mesh are presented in *Figure 3.30* and *Figure 3.31* respectively. The elements with the minimum thickness are at the top of the plate, except the one at which vertical point load is applied. This is due to the cancelling effect of compressive stress due to uniaxial compression and tensile stress due to the point load on these nodes. The stress-strain state in the plate and position of element with maximum thickness is highly dependent upon the proportions of the applied loads. It is found that the element with maximum thickness is thicker when multiple loads are applied than in case of adding the thicknesses for the same element

by applying different loads separately. The decrease of strain with increasing iteration loops is shown in *Figure 3.32*. The load case is also tried with 100% growth rate and it takes one increment loop to converge. The result of thickness distribution is presented as *Figure 3.33*.

5 Discussion and Conclusions

The algorithm developed in this thesis optimises the ply orientation and its thickness according to the stress state in the structure. The structure is optimised for quasi-static conditions and not for dynamic loading such as fatigue and vibration loads. Since classical laminate theory is used to model the composite material, only in-plane deformations are considered. As a consequence, the method is unable to consider the influence of out-of-plane stresses, free edge effects and delamination at the free edges due to large interlaminar shear stresses. Although the maximum strain failure criterion is used as a design constraint, principal stresses are used to increase the ply thickness. The reason is that for unidirectional cases the stresses in the second principal direction is zero. Hence, if the principal stresses alone are used to increase the ply thickness, no ply will be added along the second principal direction. However, based on strains, the algorithm will consider the non-energy strains in the second principal direction as well and add plies in that direction. It is also observed that, for a general stress state, if principal strains are used to increase ply thickness, the amount of plies added along the main direction decreases and increases in the other direction.

The algorithm is sensitive to the rate of increase in thickness, especially in the beginning when the first anisotropic ply is introduced, since the principal stresses in an isotropic material are compared with composite strength. Except for the case of uniaxial tension, when a growth factor of 100% is used to increase ply thickness, the final thickness of the individual elements is higher and final strains are much lower than the failure criteria. The reason is that extra material is added during each increment loop. It should be noted that, in case of 100% thickness increments with respect to the initial stress state, apart from uniaxial loading cases, the convergence took more than one step for the rest of the load cases. If instead of thickness of the element in the previous step,t_{n-1}, thickness of the isotropic layer, t_{iso}, is used in evolution, the results obtained are more refined. However this will make the algorithm computationally very expensive.

Due to shear locking, the results are affected when large shear stresses are present in the structure as in the case of pure shear; See also Section 3.4. In case of mixed loading the thickness obtained dependent upon the overall stress distribution of the structure. This could possibly the reason that the thickness of the most loaded element

in the mixed mode is not equal to the sum of thicknesses for the same element when the loads are applied separately; See Sections 3.1, 3.2 and 3.6.

From above discussion it can be concluded that

1. The algorithm has a linear convergence, i.e. C^0 convergence
2. Reasonable results are obtained for different loading cases
3. It is sensitive to the initial thickness of the isotropic layer
4. Growth factor has an important effect on final results
5. Element type effects the thickness distribution of the element
6. Results for mixed loading are different from the case when loads are applied separately
7. Linear convergence make the algorithm computationally expensive, especially for complicated problems
8. Number of iterations depend upon the load for a particular case
9. Computation time for a particular case with a given load depends upon the number of elements
10. One way to avoid long calculation time could be to calculate thickness distribution for small loads and scale them for larger loads

6 Future work

Based on the discussion and conclusions some areas of future work are recommended. Test could be conducted to validate the results obtained from algorithm. Element exclusion and re-meshing can give more refined results. More accurate calculation of transverse modulus and in-plane shear can be done using empirical model like Halpin-Tsai. This will result in better results in form of less ply thickness in a given direction. Use of higher order composite theories to incorporate shear deformation between composite layers and transverse shear strain in the calculations like first order shear deformation theory. Use of higher order plate or shell elements to considers the out-of-plane deformations. Use of such elements and with higher order composite theories will determine the stress-strain state more accurately for complicated load cases and thus improve the results. This algorithm could be used as adhoc method to calculate ply thickness using 100% growth rate. As seen from the convergence plots the decrease in maximum absolute strain is faster in the beginning of the algorithm. It is also noticed that the principal stress direction for highly stressed elements doesn't change with increase in ply thickness. Thus the thickness distribution for first 20-40 iterations with constant ply angles can be used as an initial guess for finding an optimum thickness distribution using a gradient method. Once the algorithm is matured enough it can be imbedded in a fibre/tape placement equipment to place tows on a base material.

References

1. Gill, P.E., Murray, W., Wright, M.H. (1983): Practical Optimization. Academic Press, London, United Kingdom.
2. Reklitis, G.V., Ravindran, A., Ragsdell, K.M. (1983): Engineering Optimization, Methods and Applications. Willey-Interscience publication, United States of America.
3. Belegundu, A.D., Chandrupatla, T.R., (1999): Optimization Concepts and Applications in Engineering. Prentice-Hall, New Jersey, United States of America.
4. Andreasson, N., Evgrafov, A., Patriksson, M., (2005): An introduction to continuous optimization: foundation and fundamental algorithms. Studentlitteratur, Lund, Sweden
5. Walsh, G.R., (1975): Methods of Optimization. Willey-Interscience publication, Bath, England.
6. Lundgren, J., Rönnqvist, M., Värbrand, P., (2010): Optimization. Studentlitteratur, Lund, Sweden.
7. Setoodeh. S., Abdalla, M. M., Gurdal, Z. (2006): Design of variable-stiffness laminates using lamination parameters. Composites Part B, Vol. 37, Issue 4-5, pp. 301-309.
8. Hermann. D. (2008): Genetic optimisation of tow placement in composite structures with stress concentrations. Master thesis. Institute of Aircraft Design, University of Stuttgart, Stuttgart Germany.
9. Topal, U., Uzman, U. (2008): Maximization of buckling of laminated composite plates with central circular holes using MFD method. Structural and Multidisciplinary Optimization, Vol. 45, No. 2, pp. 131-139.
10. Topal, U., Uzman, U. (2010): Modified feasible direction. Finite elements in analysis and design, Vol. 46, pp. 273-279.
11. Lindgaard, E., Lund, E. (2011): A unified approach to nonlinear buckling optimization of composite structures. Computers and Structures, Vol. 89, pp. 357-370.
12. Akbulut, M., Sonmez, F. O. (2008): Optimum design of composite laminates for minimum thickness. Computers and Structures, Vol. 86, Issue 21-22, pp. 1974-1982.
13. Naik, G. N., Gopalakrishnan, S., Ganguli, R.(2008): Design optimization of composites using genetic algorithms and failure mechancism based failure criterion. Composite Structures, Vol. 83, pp. 354-367.
14. Legrand, X., Kelly, D., Crosky, A., Crepin, D. (2006): Optimisation of fibre steering in composite laminates using a genetic algorithm. Composite Structures, Vol. 75, pp. 524-531.
15. Almeida, F. S., Awrusch, A. M. (2009): Design optimization of composite laminated structures using genetic algorithms and finite element analysis. Composite Structures, Vol. 88, pp. 443-454.

16. Paluch, B., Grediac, M., Faye, A. (2008): Combining a finite element programme and genetic algorithm to optimize composite structures with variable thickness. Composite Structures, Vol. 83, pp. 284-294.
17. Whitley, D. (1994): A genetic algrothim tutorial. Statistics and Computing, Vol.4, pp. 65-85.
18. Kaw, A. K. (2006): Mechanics of composite materials, 2nd edition. CRC press, Taylor & Francis Group, Boca Raton, USA.
19. Kollar, L. P., Springer, G. S. (2003): Mechanics of composite materials. Cambridge University Press, Cambridge, United Kingdom.
20. Rychwalski, R., Li, C. (2010): Composite and Nanocomposite materials. Course compendium 4th edition. Chalmers University of Technology, Göteborg Sweden.
21. CALFEM version 3.4 manual, 2004. Division of structural mechanics, Lund University.
22. Ottosen, N., Petersson, H., (1992): Introduction to the finite element methods. Pearson Education Limited, Dorchester Great Britain.
23. Ochoa, O. O., Reddy, J. N. (1992): Finite element analysis of composite laminates. Kluwer Academic Publishers, Dordrecht The Netherlands.
24. Matthews, F. L., Davies, G. A. O., Hitchings, D., Soutis, C. (2000): Finite element modelling of composite materials and structures. CRC Press, Woodhead Publishing Limited, Cambridge England.